IFT-UAM/CSIC-00-09
MADPH-00-1158
hep-ph/0003246

Complete Two-loop Dominant Corrections to the Mass of the Lightest $\mathcal{CP}$-even Higgs Boson in the Minimal Supersymmetric Standard Model

Jose Ramón Espinosa[a], Ren-Jie Zhang[b]

[a] *Instituto de Matemáticas y Física Fundamental (CSIC)*
Serrano 113 bis, 28006 Madrid, SPAIN
[b] *Department of Physics, University of Wisconsin*
1150 University Avenue, Madison Wisconsin 53706, USA
`espinosa@makoki.iem.csic.es, rjzhang@pheno.physics.wisc.edu`

Abstract

Using an effective potential approach, we compute two-loop radiative corrections to the MSSM lightest $\mathcal{CP}$-even Higgs boson mass M_{h^0} to $\mathcal{O}(\alpha_t^2)$ for arbitrary left-right top-squark mixing and $\tan\beta$. We find that these corrections can increase M_{h^0} by as much as 5 GeV; assuming a SUSY scale of 1 TeV, the upper bound on the Higgs boson mass is $M_{h^0} \approx 129 \pm 5$ GeV for the top quark pole mass 175 ± 5 GeV. We also derive an analytical approximation formula for M_{h^0} which is good to a precision of $\lesssim 0.5$ GeV for most of the parameter space and suitable to be further improved by including renormalization group resummation of leading and next-to-leading order logarithmic terms. Our final compact formula admits a clear physical interpretation: radiative corrections up to the two-loop level can be well approximated by a one-loop expression with parameters evaluated at the appropriate scales, plus a smaller finite two-loop threshold correction term.

March, 2000

1 Introduction

It is difficult to overestimate the importance of the experimental discovery of the Higgs boson. It would not only help us to elucidate the dynamics responsible for electroweak symmetry breaking but it will most probably offer also an important clue as to the nature of the Physics beyond the Standard Model (SM).

The paradigm for this new Physics, granted that a fundamental scalar drives electroweak symmetry breaking, is the Minimal Supersymmetric Standard Model (MSSM) [1]: the most economical extension of the Standard Model that incorporates (softly-broken) Supersymmetry (SUSY). In spite of the uncertainties related to the origin of supersymmetry breaking (and therefore of the masses of the so far undetected supersymmetric particles), it is well known that the MSSM predicts the existence of a light Higgs particle with mass below about 135 GeV (this bound depends sensitively on the top quark mass one uses; our present calculation intends to set a precise and firm bound). Unlike the case of the Standard Model (in which the mass of the Higgs boson is an unknown parameter), the mass of the light $\mathcal{CP}$-even Higgs boson of the MSSM is calculable as a function of other masses of the model. A precise calculation of that mass is of prime importance for Higgs searches at LEP, Tevatron and the LHC, and is the topic of this paper.

We recall at this point that the Higgs sector of the MSSM consists of two $SU(2)$ doublets, H_1 (which gives mass to down-type quarks and charged leptons) and H_2 (which gives mass to up-type quarks). The vacuum expectation values ($v_{1,2}$) of these doublets break the electroweak symmetry, after which, the Higgs spectrum contains two $\mathcal{CP}$-even scalars (h^0 and H^0; with $m_{h^0} \leq m_{H^0}$), one $\mathcal{CP}$-odd pseudoscalar (A^0) and a pair of charged Higgses ($H^{\pm}$). At tree-level, the masses, couplings and mixing angles of these particles are determined by one unknown mass parameter (say m_{A^0}) and the parameter β, which measures the ratio $v_2/v_1 (\equiv \tan\beta)$. In the limit $m_{A^0} \gg M_Z$ all the Higgs particles except h^0 have masses $\sim m_{A^0}$ and rearrange in a complete $SU(2)$ doublet almost decoupled from electroweak symmetry breaking, while h^0 remains light with $m_{h^0}^2 \leq M_Z^2 \cos^2 2\beta$ and has SM properties. This bound (which applies for any value of m_{A^0} and is saturated for $m_{A^0} \gg M_Z$) is extremely important: it represents the limit that experimental bounds should reach to falsify the MSSM. In fact, the present experimental bound [2] from LEP, including the latest data with up to $\sqrt{s} = 202$ GeV, is $m_{h^0} \gtrsim 107.7$ GeV (for large m_{A^0}, case in which the SM limit is applicable; the limit falls to ~ 91 GeV for smaller m_{A^0}), which is well above this bound. This is not yet conclusive evidence against the MSSM because it does not take into account the radiatively corrected form of the mass bound.

Radiative corrections to $m_{h^0}^2$ have been computed using three different techniques (or combinations of them): effective potential method [3, 4, 5, 6, 7], direct diagrammatic calculation [8, 9, 10] and effective theory (or renormalization group) approach [4, 7, 11, 12, 13]. The full one-loop radiative corrections to m_{h^0} have been computed diagrammatically. The most important of these corrections come from top quark/squark loops and are given by

$$\Delta m_{h^0}^2 = \frac{3m_t^4}{2\pi^2 v^2} \ln \frac{m_{\tilde{t}}^2}{m_t^2} , \tag{1}$$

where m_t is the top quark mass, $m_{\tilde{t}}$ an average top-squark mass and $v^2 \equiv v_1^2 + v_2^2 = (246\ \text{GeV})^2$. This correction can be very large if $m_{\tilde{t}} \gg m_t$, and in such case m_{h^0} can evade easily the current experimental lower bound. This important $\mathcal{O}(\alpha_t)$ logarithmic correction to the dimensionless ratio $m_{h^0}^2/m_t^2$ [here $\alpha_t \equiv h_t^2/(4\pi)$, where h_t is the top-quark Yukawa coupling] can be most easily reproduced using renormalization group (RG) techniques. In addition, there is a finite (non-logarithmic) correction which may also be important, and which depends on the details of the top-squark spectrum. This correction is (assuming again for simplicity degenerate soft masses for the top-squarks)

$$\Delta m_{h^0}^2 = \frac{3m_t^4}{2\pi^2 v^2}\left(\frac{X_t^2}{m_{\tilde{t}}^2} - \frac{X_t^4}{12m_{\tilde{t}}^4}\right) , \tag{2}$$

where $X_t = A_t + \mu\cot\beta$ is the top-squark mixing parameter, A_t the soft trilinear coupling associated to the top-Yukawa term in the superpotential and μ the supersymmetric Higgs mass parameter. Correction (2) is maximized for $X_t^2 = 6m_{\tilde{t}}^2$ (the so-called 'maximal-mixing' case). When using one-loop equations like (1) and (2) to compute the Higgs mass one has to decide whether to use on-shell (OS) or running values for the mass parameters that enter such formulae (and if the latter, at which scale to evaluate them). The difference between two such choices is of higher order, but can be non-negligible, especially because of the m_t^4-dependence of $\Delta m_{h^0}^2$. Although RG techniques can be used to make an educated guess of the scale at which those mass parameters should be evaluated (see *e.g.* [12]), a precise answer to such questions could only be unambiguously given by a two-loop calculation like the one we perform in this paper.

At two loops, radiative corrections to $m_{h^0}^2$ depend not only on the large top-Yukawa coupling but also on the QCD coupling g_3. It is reasonable to expect that the dominant two-loop corrections will be of order $\mathcal{O}(\alpha_s\alpha_t[\ln(m_{\tilde{t}}^2/m_t^2)]^k)$ and $\mathcal{O}(\alpha_t^2[\ln(m_{\tilde{t}}^2/m_t^2)]^k)$, $k = 0, 1, 2$. Terms with $k = 2$ are the two-loop leading logarithmic contributions and can be obtained by RG techniques using one-loop RG equations; no true two-loop calculation is required and RG resummation will take into account such leading-logarithmic (LL) corrections to all loops. The $k = 1$ terms are the two-loop next-to-leading-logarithmic (NTLL) corrections, which can be obtained (and resummed to all loops) with two-loop RG equations. Finally, the two-loop non-logarithmic terms ($k = 0$) can be interpreted in the effective theory language as threshold corrections (at the supersymmetric scale set by the mass of the top-squarks) and require a genuine two-loop calculation; they simply cannot be obtained from RG arguments.

The status of these higher-loop calculations of the radiatively corrected $m_{h^0}^2$ is the following. Higher-order logarithmic corrections were included in studies which used RG techniques almost since the dramatic impact of radiative corrections on m_{h^0} was first recognized. Hempfling and Hoang [5] were the first to perform a genuine two-loop calculation of m_{h^0} which also included non-logarithmic terms. They computed the dominant two-loop radiative corrections [to $\mathcal{O}(\alpha_s\alpha_t)$ and $\mathcal{O}(\alpha_t^2)$] in the case $\tan\beta \gg 1$ and zero top-squark mixing. Their computation also included the most important logarithmic corrections, which could be alternatively incorporated by RG resummation from one-loop results, as done *e.g.* in Ref. [4]. In this last paper it was also pointed out that by a judicious choice of the renormalization scale at which to evaluate one-loop corrections, the higher order logarithmic corrections could be automatically taken into account. A similar idea was later implemented in [12, 13] to write down simple analytical approximations for the radiatively corrected $m_{h^0}^2$, obtained by iterative integration of RG equations.

Besides being limited to a particularly simple value of $\tan\beta$, the calculation in Ref. [5] missed the sizable impact of non-zero top-squark mixing in two-loop effects, that is, higher order corrections to the contribution written down in Eq. (2). Such corrections were first included to order $\mathcal{O}(\alpha_s\alpha_t)$ in the diagrammatic calculation [9], and by the effective potential method in Ref. [6].

The effect of these corrections is to shift the values of X_t that give maximal mixing, change the corresponding Higgs mass by up to ~ -10 GeV* and introduce an asymmetry in the dependence of m_{h^0} with the sign of X_t. This two-loop top-squark mixing dependent correction was also explicitly isolated recently by the present authors in Ref. [7], which uses effective potential plus RG techniques. Besides confirming the independent diagrammatic results of Ref. [9] we clarified the relation of these calculations to previous ones (in particular matching results expressed in different renormalization schemes; see also [14]). We also derived a compact formula for the Higgs mass (in the spirit of [12, 13]) which took into account the most important radiative corrections, and used RG techniques to include in a compact way two-loop LL and NTLL corrections. With the $\mathcal{O}(\alpha_s\alpha_t)$ radiative corrections organized in this way, we find that the mixing-dependent genuine two-loop threshold corrections are generally small ($\lesssim 3$ GeV).

Nevertheless, the large computing effort just reviewed did not exhaust the potentially important radiative corrections: the two-loop $\mathcal{O}(\alpha_t^2)$ top-squark-mixing-dependent corrections to m_{h^0} remained unknown to this day, while it is clear that they could compete in principle with the $\mathcal{O}(\alpha_s\alpha_t)$ contributions. The purpose of this paper is to complete the calculation performed in [5, 6, 7] by using effective potential techniques (plus RG techniques) to compute such $\mathcal{O}(\alpha_t^2)$ contributions for general top-squark mixing parameters and any value of $\tan\beta$. The results in this paper can be considered the most complete and accurate approximation to m_{h^0} presented in the literature.

The structure of the paper is the following: the next Section describes the strategy of our calculation and presents some analytical formulae for m_{h^0}, obtained in the limit of $m_{\tilde{t}} \gg m_t$. Section 3 goes one step ahead implementing the RG-improvement of such approximations and, in doing so, clarifies the organization of the higher order radiative corrections. This procedure is not only important to provide a clearer physical picture in connection with the effective field theory but also to classify those corrections calculated in Sec. 2 into a numerically dominant and compact part plus smaller finite threshold correction terms. In Section 4 we present our numerical results for the Higgs mass, illustrate the size of the new corrections and check the validity of our analytical approximation formulae. We draw some conclusions in Section 5.

Several appendices are devoted to technical details of different aspects of the calculation. Appendix D is worth special mention as it contains the two-loop $\mathcal{O}(\alpha_t^2)$ MSSM effective potential used as starting point of our calculation and first computed in this paper.

2 $\mathcal{CP}$-even Higgs boson masses to two-loop order

The momentum-dependent mass-squared matrix for the $\mathcal{CP}$-even Higgs bosons of the MSSM in the interaction eigenstate basis $h_1,\ h_2$ is

$$\mathcal{M}_h^2(p^2) \;=\; \left[\begin{array}{cc} m_Z^2 c_\beta^2 + m_{A^0}^2 s_\beta^2 + \Delta\mathcal{M}_{11}^2(p^2) & -(m_Z^2+m_{A^0}^2)s_\beta c_\beta + \Delta\mathcal{M}_{12}^2(p^2) \\ -(m_Z^2+m_{A^0}^2)s_\beta c_\beta + \Delta\mathcal{M}_{21}^2(p^2) & m_Z^2 s_\beta^2 + m_{A^0}^2 c_\beta^2 + \Delta\mathcal{M}_{22}^2(p^2) \end{array}\right] , \qquad (3)$$

where $s_\beta \equiv \sin\beta$ and $c_\beta \equiv \cos\beta$. The mass parameters m_Z and m_{A^0} are the (scale-dependent) running masses of the Z-boson and $\mathcal{CP}$-odd Higgs boson A^0; they are related to the on-shell masses

*This correction is relative to the one-loop mass using on-shell parameters. The size of the correction would be much smaller if running parameters are used in the one-loop formula (1).

M_Z and M_{A^0} (we use capital letters to distinguish on-shell parameters from running ones) by

$$m_Z^2 \ = \ M_Z^2 + \mathrm{Re}\ \Pi_{ZZ}^T(M_Z^2) \ , \qquad m_{A^0}^2 \ = \ M_{A^0}^2 + \mathrm{Re}\ \Pi_{AA}(M_{A^0}^2) - s_\beta^2 \frac{T_1}{v_1} - c_\beta^2 \frac{T_2}{v_2} \ , \tag{4}$$

where Π_{ZZ}^T is the transverse part of the Z-boson self-energy and Π_{AA} the A^0-boson self-energy, $T_1,\ T_2$ are the tadpoles of the $\mathcal{CP}$-even (real) fields $h_1,\ h_2$. Their explicit one-loop expressions can be found *e.g.* in Ref. [10].

In (3), $\Delta\mathcal{M}^2$ stands for the contributions from radiative corrections. They are

$$\Delta\mathcal{M}_{ij}^2(p^2) \ = \ -\Pi_{ij}(p^2) + \frac{T_i}{v_i}\delta_{ij} \ , \qquad i,j = 1,2 \ , \tag{5}$$

where Π_{ij} is the self-energy matrix of the Higgs fields h_1 and h_2. The masses, m_{h^0}, m_{H^0}, of the two $\mathcal{CP}$-even Higgs bosons are then obtained from the real part of the poles of the propagator matrix,

$$\mathrm{Det}\left[m_{h^0,H^0}^2 \mathbf{1} - \mathcal{M}_h^2(m_{h^0,H^0}^2)\right] \ = \ 0 \ . \tag{6}$$

The radiatively corrected mixing angle α is obtained as the angle of that rotation which diagonalizes $\mathcal{M}_h^2$ (for some choice of p^2, say $p^2 = m_{h^0}^2$):

$$\tan 2\alpha = \frac{2(\mathcal{M}_h^2)_{12}}{(\mathcal{M}_h^2)_{11} - (\mathcal{M}_h^2)_{22}} \ . \tag{7}$$

Computing Higgs boson masses to a certain order of perturbation theory then requires calculating the self-energies and tadpoles in Eqs. (4) and (5) to that order.

In the effective potential approach [3, 4, 5, 6, 7], self-energies and tadpoles can be calculated as derivatives of the Higgs potential V according to:

$$T_i \ = \ - \left[\frac{\partial V(h_1,h_2)}{\partial h_i}\right]\Bigg|_{h_1=v_1,h_2=v_2} \ , \qquad \Pi_{ij}(0) \ = \ - \left[\frac{\partial^2 V(h_1,h_2)}{\partial h_i \partial h_j}\right]\Bigg|_{h_1=v_1,h_2=v_2} \ . \tag{8}$$

Note that the Π's obtained from derivatives of V have zero external momentum.

In the limit $M_{A^0} \gg M_Z$, the lightest $\mathcal{CP}$-even Higgs state lies along the direction of the breaking in field space [15], that is, $\alpha \to \beta - \pi/2 + \mathcal{O}(m_Z^2/m_A^2)$, and its radiatively corrected mass has a very simple expression

$$M_{h^0}^2 \ = \ \frac{4m_t^4}{v^2}\left(\frac{d}{dm_t^2}\right)^2 V - \mathrm{Re}\ \Pi_{hh}(m_{h^0}^2) + \mathrm{Re}\ \Pi_{hh}(0) \ , \tag{9}$$

which is exact up to corrections of order $\mathcal{O}(m_Z^4/m_{A^0}^2)$.[†]

In Eq. (9), V is the projection of $V(h_1,h_2)$ along the light Higgs $h = h_1 c_\beta + h_2 s_\beta$: $V(h) = V(h_1 \to h c_\beta, h_2 \to h s_\beta)$. Then $V(h)$ can be expressed as a function of m_t using $h \to m_t\sqrt{2}/(h_t s_\beta)$.

[†]This formula can be proved as follows: If $m_{A^0}^2 \gg m_Z^2$, $\alpha \to \beta - \pi/2$, and we can therefore use the approximation $\Delta m_{h^0}^2 \simeq \Delta\mathcal{M}_{11}^2 c_\beta^2 + \Delta\mathcal{M}_{22}^2 s_\beta^2 + 2\Delta\mathcal{M}_{12}^2 s_\beta c_\beta$, up to higher order terms in $m_Z^4/m_{A^0}^2$. Observing that the potential V depends on the fields h_1 and h_2 only through (field-dependent) top quark mass and the off-diagonal elements of the top-squark mass-squared matrix and using (8), we can easily express the partial derivatives of V in terms of the total derivative in (9). A similar formula was already used in [5].

We decompose V in its n^{th}-loop pieces V_n (explicitly given in Appendix D) as $V = V_0 + V_1 + V_2$. The tree-level part V_0 is the only one in which we keep non-zero electroweak gauge couplings. We approximate the one-loop part V_1 by its $\mathcal{O}(\alpha_t)$ piece coming from top quark/squark loops. The two-loop part V_2 is approximated by $V_{2s} + V_{2t}$, where V_{2s} is the $\mathcal{O}(\alpha_s\alpha_t)$ part and V_{2t} the $\mathcal{O}(\alpha_t^2)$ one.

Next, $\Pi_{hh}(p^2)$ is the light Higgs self-energy at external momentum p, related to the self-energies of $h_{1,2}$ by

$$\Pi_{hh}(p^2) \equiv \Pi_{11}(p^2)s_\alpha^2 + \Pi_{22}(p^2)c_\alpha^2 - 2\Pi_{12}(p^2)s_\alpha c_\alpha \ . \tag{10}$$

Notice that the self-energy difference in (9) involves non-zero external momentum and would require a diagrammatic two-loop calculation. However, throughout this paper we work in the approximation of neglecting in the radiative corrections all couplings other than h_t or g_3. In that case, realizing that at tree level m_{h^0} depends only on electroweak gauge couplings while its dependence on h_t appears only at one-loop, we can write

$$\Pi_{hh}(m_{h^0}^2) - \Pi_{hh}(0) \simeq m_{h^0}^2 \left. \frac{d}{dp^2}\Pi_{hh}(p^2)\right|_{p^2=0} \ , \tag{11}$$

which gives rise to $\mathcal{O}(\alpha_t^2)$ contributions from the one-loop $\mathcal{O}(\alpha_t)$ self-energy Π_{hh}.

In Section 4 we present the numerical results of such procedure for the two-loop potential with $\mathcal{O}(\alpha_s\alpha_t)$ and $\mathcal{O}(\alpha_t^2)$ corrections included. The general expression for the $\mathcal{O}(\alpha_s\alpha_t)$ potential was first computed in [6] while the complete $\mathcal{O}(\alpha_t^2)$ terms were still missing. Both contributions to V are given in Appendix D.

It is useful, both for a better understanding of the numerical results and for practical applications, to derive an analytical expression for the light Higgs mass in the case of a large hierarchy between the supersymmetric scale and the electroweak scale (say when the SUSY scale is of order 1 TeV). Such limit is interesting because it maximizes the radiative corrections to $m_{h^0}^2$ (so that it corresponds to the most pessimistic scenario for Higgs searches; the case one should be able to discard to rule out the MSSM), and at the same time simplifies the structure of the radiative corrections, avoiding the proliferation of a multitude of different supersymmetric thresholds.

We consequently assume now that all supersymmetric particles have roughly the same mass $M_S \gg M_Z$. In more detail, focusing on the particles relevant for the radiative corrections to m_{h^0}, we take equal soft masses $M_{\widetilde{Q}} = M_{\widetilde{U}} = M_S$ for the top-squarks (with diagonal masses $m_{\tilde{t}}^2 \simeq M_S^2 + m_t^2$). The two eigenvalues and mixing angle of the top-squark squared-mass matrix are then

$$m_{\tilde{t}_1}^2 \ = \ m_{\tilde{t}}^2 + m_t X_t \ , \qquad m_{\tilde{t}_2}^2 \ = \ m_{\tilde{t}}^2 - m_t X_t \ , \qquad s_t^2 \ = \ c_t^2 \ = \ \frac{1}{2} \ , \tag{12}$$

We also take the same mass M_S for the gluino and the pseudoscalar Higgs [this means in particular that we can use Eq. (9) for the light Higgs boson]. In principle we admit the possibility that the μ parameter could be smaller than M_S, in which case we expect that one chargino and two neutralinos will have masses $\sim |\mu|$ below the common supersymmetric threshold. In this situation, which broadly corresponds to the case of a common heavy SUSY scale, we find that, using the operator

$$\mathcal{D}_m^2 \equiv \frac{4m_t^4}{v^2}\left(\frac{d}{dm_t^2}\right)^2 , \tag{13}$$

the different parts entering (9) are

$$\begin{aligned}
\mathcal{D}^2_m V_0 &= m_Z^2 \cos^2 2\beta, && (14)\\
\mathcal{D}^2_m V_1 &= \frac{3m_t^4}{2\pi^2 v^2}\Big(\ln\frac{M_S^2}{m_t^2} + \hat{X}_t^2 - \frac{\hat{X}_t^4}{12}\Big), && (15)\\
\mathcal{D}^2_m V_{2s} &= \frac{\alpha_s m_t^4}{\pi^3 v^2}\Big\{\ln^2\frac{M_S^2}{m_t^2} - 2\ln^2\frac{M_S^2}{Q^2} + 2\ln^2\frac{m_t^2}{Q^2} + \ln\frac{m_t^2}{Q^2} - 1 + \Big(-1 + 2\ln\frac{M_S^2}{Q^2} + 2\ln\frac{m_t^2}{Q^2}\Big)\hat{X}_t \\
&\qquad + \Big(1 - 2\ln\frac{M_S^2}{Q^2}\Big)\Big(\hat{X}_t^2 + \frac{\hat{X}_t^3}{3}\Big) - \frac{\hat{X}_t^4}{12}\Big\}, && (16)\\
\mathcal{D}^2_m V_{2t} &= \frac{3\alpha_t m_t^4}{16\pi^3 v^2}\Big\{9\ln^2\frac{M_S^2}{Q^2} - 6\ln\frac{m_t^2}{Q^2}\ln\frac{M_S^2}{Q^2} - 3\ln^2\frac{m_t^2}{Q^2} + 2[3f_2(\hat{\mu}) - 3f_1(\hat{\mu}) - 8]\ln\frac{M_S^2}{m_t^2} \\
&+ 6\hat{\mu}^2\Big(1 - \ln\frac{M_S^2}{Q^2}\Big) - 2(4+\hat{\mu}^2)f_1(\hat{\mu}) + 4f_3(\hat{\mu}) - \frac{\pi^2}{3} \\
&+ \Big[(33 + 6\hat{\mu}^2)\ln\frac{M_S^2}{Q^2} - 10 - 6\hat{\mu}^2 - 4f_2(\hat{\mu}) + (4 - 6\hat{\mu}^2)f_1(\hat{\mu})\Big]\hat{X}_t^2 \\
&+ \Big[-4(7+\hat{\mu}^2)\ln\frac{M_S^2}{Q^2} + 23 + 4\hat{\mu}^2 + 2f_2(\hat{\mu}) - 2(1-2\hat{\mu}^2)f_1(\hat{\mu})\Big]\frac{\hat{X}_t^4}{4} \\
&+ \frac{1}{2}s_\beta^2\hat{X}_t^6\Big(\ln\frac{M_S^2}{Q^2} - 1\Big) + c_\beta^2\Big[3\ln^2\frac{M_S^2}{m_t^2} + 7\ln\frac{M_S^2}{Q^2} - 4\ln\frac{m_t^2}{Q^2} - 3 + 60K + \frac{4\pi^2}{3} \\
&+ \Big(12 - 24K - 18\ln\frac{M_S^2}{Q^2}\Big)\hat{X}_t^2 - \Big(3 + 16K - 3\ln\frac{M_S^2}{Q^2}\Big)(4\hat{X}_t\hat{Y}_t + \hat{Y}_t^2) \\
&+ \Big(-6 + \frac{11}{2}\ln\frac{M_S^2}{Q^2}\Big)\hat{X}_t^4 + \Big(4 + 16K - 2\ln\frac{M_S^2}{Q^2}\Big)\hat{X}_t^3\hat{Y}_t \\
&+ \Big(\frac{14}{3} + 24K - 3\ln\frac{M_S^2}{Q^2}\Big)\hat{X}_t^2\hat{Y}_t^2 - \Big(\frac{19}{12} + 8K - \frac{1}{2}\ln\frac{M_S^2}{Q^2}\Big)\hat{X}_t^4\hat{Y}_t^2\Big]\Big\}, && (17)
\end{aligned}$$

The notations used are $\hat{X}_t = \hat{A}_t + \hat{\mu}\cot\beta$, $\hat{Y}_t = \hat{A}_t - \hat{\mu}\tan\beta$, with reduced parameters $\hat{z} \equiv z/M_S$, and (see Appendix A) $K \simeq -0.1953256$. We also use the following non-singular functions of $\hat{\mu}$

$$\begin{aligned}
f_1(\hat{\mu}) &= \frac{\hat{\mu}^2}{1-\hat{\mu}^2}\ln\hat{\mu}^2, \\
f_2(\hat{\mu}) &= \frac{1}{1-\hat{\mu}^2}\Big[1 + \frac{\hat{\mu}^2}{1-\hat{\mu}^2}\ln\hat{\mu}^2\Big], \\
f_3(\hat{\mu}) &= \frac{(-1 + 2\hat{\mu}^2 + 2\hat{\mu}^4)}{(1-\hat{\mu}^2)^2}\Big[\ln\hat{\mu}^2\ln(1-\hat{\mu}^2) + Li_2(\hat{\mu}^2) - \frac{\pi^2}{6} - \hat{\mu}^2\ln\hat{\mu}^2\Big], && (18)
\end{aligned}$$

with $f_1(0) = 0,\ f_2(0) = 1,\ f_3(0) = -\pi^2/6$ and $f_1(1) = -1,\ f_2(1) = 1/2,\ f_3(1) = -9/4$.

Finally, the correction for non-zero external momentum in Eq. (9) is given by (see Appendix C)

$$\mathrm{Re}\Big[-\Pi_{hh}(m_{h^0}^2) + \Pi_{hh}(0)\Big] = \frac{h_t^2}{16\pi^2}m_{h^0}^2 s_\beta^2\Big(3\ln\frac{m_t^2}{Q^2} + 2 - \frac{\hat{X}_t^2}{2}\Big). \qquad (19)$$

The parameters that appear in these expressions are running parameters, evaluated in the $\overline{\rm DR}$ -scheme and satisfy MSSM RG equations. In fact, it can be checked that the (physical) Higgs mass, given by Eq. (9), is renormalization-scale independent (up to two-loop order), as it should. This scale independence is at the root of the RG-resummation procedure discussed in the next section. It is evident that for different values of the renormalization scale, the magnitude of the two-loop corrections will change, so that it should be possible to choose the scale in such a way that the bulk of the corrections is transferred to the one-loop terms (which depend on the scale implicitly).

Therefore, the magnitude and relevance of the two-loop corrections depends on the definition of the mass parameters that enter the one-loop corrections. It is in this respect convenient to write down the two-loop expressions just obtained in the particular case in which all mass parameters in the one-loop correction are the OS ones. This is also useful to compare with explicit diagrammatic calculations. The relationships between running and OS parameters are listed in Appendix C. Using them, we obtain for the two-loop correction to $m^2_{h^0}$:

$$
\begin{aligned}
\Delta m^2_{h^0} \;=\;& \frac{\alpha_s m_t^4}{\pi^3 v^2}\left\{-3\ln^2\frac{M_S^2}{m_t^2} - 6\ln\frac{M_S^2}{m_t^2} + 6\hat{X}_t - 3\ln\frac{M_S^2}{m_t^2}\,\hat{X}_t^2 - \frac{3}{4}\hat{X}_t^4\right\} \\
+\;& \frac{3\alpha_t m_t^4}{16\pi^3 v^2}\left\{\left(3\ln^2\frac{M_S^2}{m_t^2} + 13\ln\frac{M_S^2}{m_t^2}\right)s_\beta^2 - \frac{7}{2} - \frac{\pi^2}{3} - 3\hat{\mu}^2 - (11-\hat{\mu}^2+3\hat{\mu}^4)f_1(\hat{\mu})\right. \\
& -3(1-\hat{\mu}^2)^2\ln(1-\hat{\mu}^2) + 3f_2(\hat{\mu}) + 4f_3(\hat{\mu}) + c_\beta^2\left(60K + \frac{13}{2} + \frac{4\pi^2}{3}\right) \\
& +\left[3s_\beta^2\ln\frac{M_S^2}{m_t^2} + \frac{73}{2} + 9\hat{\mu}^2 + f_1(\hat{\mu}) - 7f_2(\hat{\mu}) - c_\beta^2\left(\frac{69}{2} + 24K\right)\right]\hat{X}_t^2 \\
& +\frac{1}{6}\left[-26 - 9\hat{\mu}^2 + 3f_1(\hat{\mu}) + 3f_2(\hat{\mu}) + \frac{61}{2}c_\beta^2\right]\hat{X}_t^4 + \frac{s_\beta^2}{2}\hat{X}_t^6 \\
& +3(1-\hat{\mu}^2)\left[(2-3\hat{\mu}^2)f_1(\hat{\mu}) - (1+3\hat{\mu}^2)\ln(1-\hat{\mu}^2)\right]\left(\hat{X}_t^2 - \frac{\hat{X}_t^4}{6}\right) \\
& +c_\beta^2\left[(3-16K-\pi\sqrt{3})(4\hat{X}_t\hat{Y}_t + \hat{Y}_t^2) + \left(16K + \frac{2\pi}{\sqrt{3}}\right)\hat{X}_t^3\hat{Y}_t\right. \\
& \left.\left. +\left(-\frac{4}{3} + 24K + \pi\sqrt{3}\right)\hat{X}_t^2\hat{Y}_t^2 - \left(\frac{7}{12} + 8K + \frac{\pi}{2\sqrt{3}}\right)\hat{X}_t^4\hat{Y}_t^2\right]\right\}
\end{aligned}
\tag{20}
$$

We emphasize that this expression gives the two-loop corrections when the one-loop contribution (15) is expressed in terms of OS parameters, that is,

$$
\left[\Delta m^2_{h^0}\right]^{\rm OS}_{1-loop} = \frac{3g^2 M_t^2}{8\pi^2 M_W^2}\left[\ln\frac{M_{\tilde{t}}^2}{M_t^2} + \left(\frac{X_t^{\rm OS}}{M_{\tilde{t}}}\right)^2 - \frac{1}{12}\left(\frac{X_t^{\rm OS}}{M_{\tilde{t}}}\right)^4\right]. \tag{21}
$$

Several features of Eq. (20) are worth commenting. First, if we restrict Eq. (20) to $\tan\beta \gg 1$ and zero A_t, to compare with the result of Ref. [5], we find the same logarithmic terms. However, the $\mathcal{O}(\alpha_t^2)$ finite term is different. In particular, that term is sensitive to the value of the parameter μ, contrary to what is stated in Ref. [5]. Nevertheless, the result quoted for that finite term in Ref. [5] is inside the range we would find by varying $\hat{\mu}^2$ from 0 to 1, and the impact of this μ-dependence on the final Higgs mass is quite small.

Second, we see that radiative corrections no longer depend on A_t and μ in the combination X_t that appears through the off-diagonal entry of the top-squark mass matrix: besides the explicit dependence on the parameter μ already noticed, the quantity Y_t also introduces a different combination of A_t and μ. This dependence on Y_t originates from the $H-\tilde{t}-\tilde{b}$ and $H-\tilde{t}-\tilde{t}$ diagrams of Fig. 8.

Third, although roughly speaking the top-Yukawa correction has a small pre-factor 3/16 in comparison with the QCD correction, this does not guarantee that the new contributions will be negligible compared to the QCD one. In fact, we will see that for two-loop top-squark-mixing-dependent corrections of (20), the top Yukawa contributions have opposite signs as that of the QCD corrections and could be as much as 60% of the latter (see Fig. 6). In the next Section, we will follow RG methods and reorganize these corrections in the effective theory language, with the most important corrections of Eq. (20) reshuffled in a RG-motivated one-loop formula.

3 Renormalization group resummation

Before illustrating in Section 4 the impact of the newly computed corrections on the Higgs mass, we show in the following how the use of renormalization group techniques [11, 12, 13] allows us to write the previous complicated corrections [see Eq. (20)] in a simpler and more transparent way, while at the same time it clarifies the connection to the RG programme, which can be used to improve the precision of the mass formula by resummation of higher order corrections.

We already applied this idea in Ref. [7] to the $\mathcal{O}(\alpha_s\alpha_t)$ two-loop corrections. By a convenient (and physically well motivated) choice of the scale at which to evaluate running parameters in the one-loop mass correction one can absorb large logarithms in Eq. (20). The RG evolution of the parameters is given by the corresponding one-loop RG functions listed in Appendix B.

We use the following equations to relate supersymmetric running parameters at different scales [*cf.* Eqs. (B.17) and (B.18)]:

$$m_{\tilde{t}}^2(Q) = m_{\tilde{t}}^2(Q')\left\{1+\frac{1}{16\pi^2}\left[\frac{16}{3}g_3^2-\frac{3}{2}h_t^2\left(\hat{X}_t^2 s_\beta^2+\hat{Y}_t^2 c_\beta^2+c_\beta^2+2-2\hat{\mu}^2\right)\right]\ln\frac{Q'^2}{Q^2}\right\} , \tag{22}$$

$$X_t(Q) = X_t(Q') - \frac{1}{16\pi^2}\left[\frac{16}{3}g_3^2 M_S + 3h_t^2(X_t + X_t s_\beta^2 + Y_t c_\beta^2)\right]\ln\frac{Q'^2}{Q^2} , \tag{23}$$

where we have used $A_t = X_t s_\beta^2 + Y_t c_\beta^2$, $A_t^2+\mu^2 = X_t^2 s_\beta^2 + Y_t^2 c_\beta^2$ and $m_{H_2}^2 + \mu^2 = m_{A^0}^2 c_\beta^2$. Notice that, to the order we work, it is sufficient to use these one-loop LL approximations to the full RG evolution because we are concerned with parameters that appear in a one-loop order term.

The Standard Model $\overline{\rm MS}$ top quark mass $\overline{m}_t$ and the Higgs VEV $\overline{v}$ are related to the on-shell mass M_t and MSSM VEV v by [*cf.* Eqs. (C.2) and (C.10), from which relevant terms can be easily identified]

$$\overline{m}_t^2(Q) = M_t^2\left[1-\frac{g_3^2}{6\pi^2}\left(4-3\ln\frac{m_t^2}{Q^2}\right)+\frac{h_t^2 s_\beta^2}{32\pi^2}\left(8-3\ln\frac{m_t^2}{Q^2}\right)\right] , \tag{24}$$

$$\overline{v}^2(Q) = v^2(Q)\left[1+\frac{h_t^2 s_\beta^2}{32\pi^2}\hat{X}_t^2\right] . \tag{25}$$

We also use one-loop LL solutions of the SM RG equations to relate these parameters at different scales:

$$\overline{m}_t^2(Q) = \overline{m}_t^2(Q') \left[1 + \frac{1}{16\pi^2}\left(8g_3^2 - \frac{3}{2}h_t^2 s_\beta^2\right)\ln\frac{Q'^2}{Q^2}\right] , \tag{26}$$

$$\overline{v}^2(Q) = \overline{v}^2(Q') \left[1 + \frac{3h_t^2 s_\beta^2}{16\pi^2}\ln\frac{Q'^2}{Q^2}\right] . \tag{27}$$

Using the above equations, we find the following compact expression for the Higgs boson mass, which is one of the main results of this paper

$$M_{h^0}^2 = M_Z^2\cos^2 2\beta + \frac{3\overline{m}_t^4(Q_t)}{2\pi^2\overline{v}^2(Q_1^*)}\ln\frac{m_{\tilde{t}}^2(Q_{\tilde{t}})}{\overline{m}_t^2(Q_t')} + \Delta_{\rm th}^{(1)} m_{h^0}^2 + \Delta_{\rm th}^{(2)} m_{h^0}^2 . \tag{28}$$

The one-loop threshold correction is

$$\Delta_{\rm th}^{(1)} m_{h^0}^2 = \frac{3\overline{m}_t^4(Q_{\rm th})}{2\pi^2\overline{v}^2(Q_2^*)}\left[\hat{X}_t^2(Q_{\rm th}) - \frac{\hat{X}_t^4(Q_{\rm th})}{12}\right] , \tag{29}$$

and the two-loop threshold correction reads

$$\begin{aligned}
\Delta_{\rm th}^{(2)} m_{h^0}^2 &= \frac{\alpha_s m_t^4}{\pi^3 v^2}\left[-2\hat{X}_t - \hat{X}_t^2 + \frac{7}{3}\hat{X}_t^3 + \frac{1}{12}\hat{X}_t^4 - \frac{1}{6}\hat{X}_t^5\right] \\
&+ \frac{3\alpha_t m_t^4}{16\pi^3 v^2}\Bigg\{R_0(\hat{\mu}) + R_2(\hat{\mu})\hat{X}_t^2 + R_4(\hat{\mu})\hat{X}_t^4 - \frac{1}{2}s_\beta^2\hat{X}_t^6 \\
&+ c_\beta^2\Bigg[60K - \frac{9}{2} + \frac{4\pi^2}{3} - (3+16K)(4\hat{X}_t\hat{Y}_t + \hat{Y}_t^2) + (15-24K)\hat{X}_t^2 \\
&- \frac{25}{4}\hat{X}_t^4 + (4+16K)\hat{X}_t^3\hat{Y}_t + \left(\frac{14}{3}+24K\right)\hat{X}_t^2\hat{Y}_t^2 - \left(\frac{19}{12}+8K\right)\hat{X}_t^4\hat{Y}_t^2\Bigg]\Bigg\}.
\end{aligned} \tag{30}$$

We have used the short-hand notation

$$\begin{aligned}
R_0(\hat{\mu}) &= -\frac{9}{2} - \frac{\pi^2}{3} + 6\hat{\mu}^2 - (11+2\hat{\mu}^2)f_1(\hat{\mu}) + 3f_2(\hat{\mu}) + 4f_3(\hat{\mu}), \\
R_2(\hat{\mu}) &= -11 - \hat{\mu}^2[6 + 6f_1(\hat{\mu}) + 10f_2(\hat{\mu})], \\
R_4(\hat{\mu}) &= 6 + \hat{\mu}^2[1 + f_1(\hat{\mu}) + f_2(\hat{\mu})] .
\end{aligned} \tag{31}$$

The scales required in (28,29) are

$$\begin{aligned}
Q_t &= \sqrt{m_t m_{\tilde{t}}} , \qquad Q_t' = (m_t m_{\tilde{t}}^2)^{1/3} , \qquad Q_{\tilde{t}} = Q_{\rm th} = m_{\tilde{t}} , \\
Q_1^* &= e^{-1/3}m_t \simeq 0.7 m_t , \qquad Q_2^* = e^{1/3}m_t \simeq 1.4 m_t .
\end{aligned} \tag{32}$$

It is a non-trivial check of our calculation that the values of the scales (32) required to re-absorb the large $\ln(M_S^2/m_t^2)$ logarithms in the two-loop corrections are consistent with the ones obtained in [7] for the QCD corrections alone. We see, in particular, that the uncertainty found there in the definition of the scales Q_t' and $Q_{\tilde{t}}$ is here resolved by the need of absorbing the new radiative corrections.

We still find a somewhat complicated expression for the threshold correction $\Delta_{\rm th}^{(2)} m_{h^0}^2$, due to the fact that we have kept free the μ parameter. Expressions for the two limiting cases of heavy μ ($\mu \simeq M_S$) and light μ ($\mu \ll M_s$) can be readily derived. In both cases, the resulting threshold correction is much simpler than the general case (30) and contains no more logarithms. Explicitly, for $\mu \ll M_s$ we find

$$R_0(0) \;=\; \frac{\pi^2}{3} - \frac{3}{2}, \qquad R_2(0) \;=\; -11, \qquad R_4(0) \;=\; 6, \tag{33}$$

and for $\mu \simeq M_S$:

$$R_0(1) \;=\; 7 - \frac{\pi^2}{3}, \qquad R_2(1) \;=\; -16, \qquad R_4(1) \;=\; \frac{13}{2}. \tag{34}$$

It is perhaps convenient to make more explicit the connection between our results and those obtained in the RG approach (see, *e.g.*, Ref. [13]). To be concrete, let us assume $|\mu| = M_S$ so that all supersymmetric particles (including charginos and neutralinos) have masses of order M_S; below that scale, the effective theory is the SM. The light Higgs quartic coupling λ at M_S consists of a tree-level part plus higher-order threshold corrections which arise from the heavy decoupling supersymmetric particles, it can be evolved down to the electroweak scale, say $Q = m_t$, using the SM RGEs; at that scale λ is related to the physical Higgs mass. This procedure should reproduce all the logarithmic corrections we have found.

More explicitly, defining $\beta_\lambda \equiv d\lambda/d\ln Q^2$, we can write

$$\lambda(\mathcal{Q}_t) = \lambda(\mathcal{Q}_{\tilde t}) - \int_{Q=\mathcal{Q}_t}^{\mathcal{Q}_{\tilde t}} \beta_\lambda \; d\ln Q^2. \tag{35}$$

We use a special notation for the high and low scales between which we run λ to distinguish them from other definitions of m_t and $m_{\tilde t}$ that appear in the paper. These quantities are defined by:

$$\mathcal{Q}_t \equiv \overline{m}_t(\mathcal{Q}_t)\ , \qquad \mathcal{Q}_{\tilde t} \equiv m_{\tilde t}(\mathcal{Q}_{\tilde t})\ , \tag{36}$$

i.e., they are the running masses evaluated at a scale equal to the corresponding mass. This is the natural definition in the RG approach.

Making a loop expansion of β_λ in (35) and a further expansion around a particular value of Q (say the low energy limit of the running interval, $\mathcal{Q}_t$), we obtain to the two-loop order

$$\lambda(\mathcal{Q}_t) \simeq \lambda(\mathcal{Q}_{\tilde t}) - \left[\beta_\lambda^{(1)}(\mathcal{Q}_t) + \beta_\lambda^{(2)}(\mathcal{Q}_t)\right] \ln\frac{\mathcal{Q}_{\tilde t}}{\mathcal{Q}_t} - \frac{1}{2}\frac{d\beta_\lambda^{(1)}}{d\ln Q^2}(\mathcal{Q}_t)\ln^2\frac{\mathcal{Q}_{\tilde t}}{\mathcal{Q}_t} + \ldots \tag{37}$$

where the one- and two-loop contributions to β_λ are approximated by [neglected all couplings other than the strong gauge coupling g_3 and the SM top Yukawa coupling g_t ($\equiv h_t s_\beta$)]

$$\begin{aligned} \beta_\lambda^{(1)} &= \frac{3g_t^2}{8\pi^2}(-g_t^2 + \lambda), \\ \beta_\lambda^{(2)} &= \frac{2g_t^4}{(16\pi^2)^2}(15g_t^2 - 16g_3^2). \end{aligned} \tag{38}$$

We note that for a correct two-loop computation it is necessary to retain also the λg_t^2 term in $\beta_\lambda^{(1)}$ because λ gets one-loop contributions proportional to g_t^4. $d\beta_\lambda^{(1)}/d\ln Q^2$ can be calculated from the one-loop RG evolution of g_t

$$\frac{dg_t^2}{d\ln Q^2} = \frac{g_t^2}{32\pi^2}(9g_t^2 - 16g_3^2). \tag{39}$$

Once $\lambda(\mathcal{Q}_t)$ is obtained from (37), we extract the physical Higgs mass using the SM relation [16]:

$$\lambda(\mathcal{Q}_t)\overline{v}^2(\mathcal{Q}_t) = M_{h^0}^2\left(1 - \frac{g_t^2}{8\pi^2}\right). \tag{40}$$

This correction arises from wave-function renormalization and takes into account the fact that the physical mass is defined on-shell, and not at zero external momentum. Its physical content is therefore similar to the correction (11) in our effective potential approach.

According to (37), the large LL and NTLL corrections to $M_{h^0}^2$ arise solely from $\lambda(\mathcal{Q}_t)$. Additional radiative contributions in (40), coming from $\overline{v}^2(\mathcal{Q}_t)$ and the wave-function correction factor, affect the large logarithmic terms only through multiplication of $\lambda(\mathcal{Q}_t)$. It is therefore clear that it is enough for our purposes to know these correction factors at one-loop order. Based on this observation, we can combine both factors together using (25) to write the simpler formula

$$M_{h^0}^2 = \lambda(\mathcal{Q}_t)\overline{v}^2(\mathcal{Q}_1^*), \tag{41}$$

with $\mathcal{Q}_1^* = e^{-1/3}\mathcal{Q}_t$, in accordance with (32).

It is now straightforward to show perfect agreement of M_{h^0} as obtained from the above expression with our results (28-30). All logarithmic corrections up to two-loops are exactly reproduced while the finite part agrees if one uses as boundary condition at the SUSY scale

$$\lambda(\mathcal{Q}_{\tilde{t}}) = \frac{1}{4}(g_1^2 + g_2^2)\cos^2 2\beta + \delta_{\rm th}^{(1)}\lambda + \delta_{\rm th}^{(2)}\lambda, \tag{42}$$

with

$$\begin{aligned} \delta_{\rm th}^{(1)}\lambda &= \frac{3g_t^4(Q_{\rm th})}{8\pi^2}\left[\hat{X}_t^2(Q_{\rm th}) - \frac{\hat{X}_t^4(Q_{\rm th})}{12}\right], \\ \delta_{\rm th}^{(2)}\lambda &= \frac{\Delta_{\rm th}^{(2)} m_{h^0}^2}{v^2}. \end{aligned} \tag{43}$$

To summarize, we find full agreement between our approximate formula (28) for the Higgs boson mass and the RG-improved mass calculated in the RG (or effective theory) approach, to two-loop order. The connection to the effective theory language clarifies the origin of the different terms in (28), and rewrites them in a very convenient way, absorbing the large (logarithmic) two-loop effects in the one-loop correction and leaving behind two-loop threshold corrections which are numerically small, as we will see in the next Section. Note that this applies in particular to the sizable top-squark-mixing-dependent corrections of Eq. (20), the bulk of which is transferred to the RG-reshuffled one-loop threshold correction of Eq. (29).

Knowing the boundary condition, $\lambda(\mathcal{Q}_{\tilde{t}})$, one can integrate (35) numerically by solving a coupled set of differential equations (describing the two-loop evolution of λ, g_3, g_t), find $\lambda(\mathcal{Q}_t)$ and use (41) to get the Higgs mass. The final result will be the full RG-improved value of M_{h^0} and will resum LL and NTLL corrections to *all loops* [numerical integration includes all the terms from the expansion around $\mathcal{Q}_t$ which were neglected in (37)]. In this respect, note that our compact formula, Eq. (28), which has been found by requiring that logarithmic contributions are correctly reproduced up to two-loops only, contains in fact logarithmic corrections of higher order. It can be shown that these higher order logarithmic corrections do not match exactly the correct ones (obtained by the RG method) if we use simple one-loop approximations [like those given in Eqs. (24,25)] to evaluate the parameters in (28) at their corresponding scales. However, evaluation of those parameters by means of a full numerical integration [similar to that in Eq. (35) for λ] would correctly take into account the LL (but not the NTLL) terms to all loops. Nevertheless, as we will see in the next Section, the error made in neglecting logarithmic corrections of higher order is very small for SUSY scales of interest [below $M_S \sim \mathcal{O}(1)$ TeV]. If M_S turns out to be significantly larger than that (starting to be in conflict with naturalness criteria), then one should revert to the numerical RG integration of λ to get a reliable estimate of the Higgs mass. Our results for the boundary condition $\lambda(\mathcal{Q}_{\tilde{t}})$ will still be useful in such a case.

4 Numerical results

In this section we present numerical results from our two-loop study. For the one-loop analysis we closely follow Ref. [10], which has included complete radiative corrections from the dominant top quark/squark sector and the sub-dominant gauge/Higgs boson and neutralino/chargino sectors. In what follows, we shall concentrate on two-loop radiative corrections.

We start by sketching the procedure for this analysis, which is the following: we first take as inputs the on-shell mass parameters[‡] M_{A^0}, M_t, $M_{\widetilde{Q}}^{\rm OS}$, $M_{\widetilde{U}}^{\rm OS}$ and $A_t^{\rm OS}$. From them we can determine the values of the corresponding running parameters at any renormalization scale Q. To do this, we have to calculate the one-loop self-energy diagrams for Higgses and top-squarks (the latter are collected in Appendix C). We also input $\tan\beta$ and μ parameters, and convert $\alpha_s(M_Z) = 0.118$ to the MSSM $\overline{\rm DR}$ running value. Next we calculate in the MSSM the two-loop corrections to the $\mathcal{CP}$-even Higgs mass matrix, $\Delta\mathcal{M}^2_{ij}$, from the two-loop potential (D.5) and (D.6) using Eq. (8). Numerically, the partial derivatives in these equations are replaced by finite differences in h_1, h_2, *i.e.* we vary the values of these fields by a finite amount and recalculate the field-dependent top-quark mass $m_t^2 = \frac{1}{2}h_t^2 h_2^2$ and top-squark masses $m_{\tilde{t}_1}$, $m_{\tilde{t}_2}$, mixing angle $\theta_{\tilde{t}}$ from Eq. (B.5). With these new parameters, the two-loop potential is reevaluated and their variations from the reference values [calculated at $h_1^2 + h_2^2 = (246\ \text{GeV})^2$] are found. Finally, equipped with the corrections $\Delta\mathcal{M}^2_{ij}$, we compute the lightest $\mathcal{CP}$-even Higgs boson mass by solving Eq. (6).

Several approximations have been made to quantities in Eqs. (3-5), in particular we neglect all dimensionless couplings other than the top-Yukawa coupling h_t and the QCD gauge coupling g_3. In this way we pick up the dominant radiative effects only, what we term throughout leading corrections. We notice that the two-loop self-energy of the Z-boson and the non-zero external momentum corrections to two-loop Higgs boson self-energies can be neglected in our calculation since all these corrections are higher order effects in the leading approximation. However, we need to calculate Π_{AA} to the two-loop level since it has $\mathcal{O}(\alpha_s\alpha_t)$ and $\mathcal{O}(\alpha_t^2)$ corrections and in principle

[‡]For the top-squark sector, we can alternatively take as inputs the on-shell top-squark masses and mixing angle.

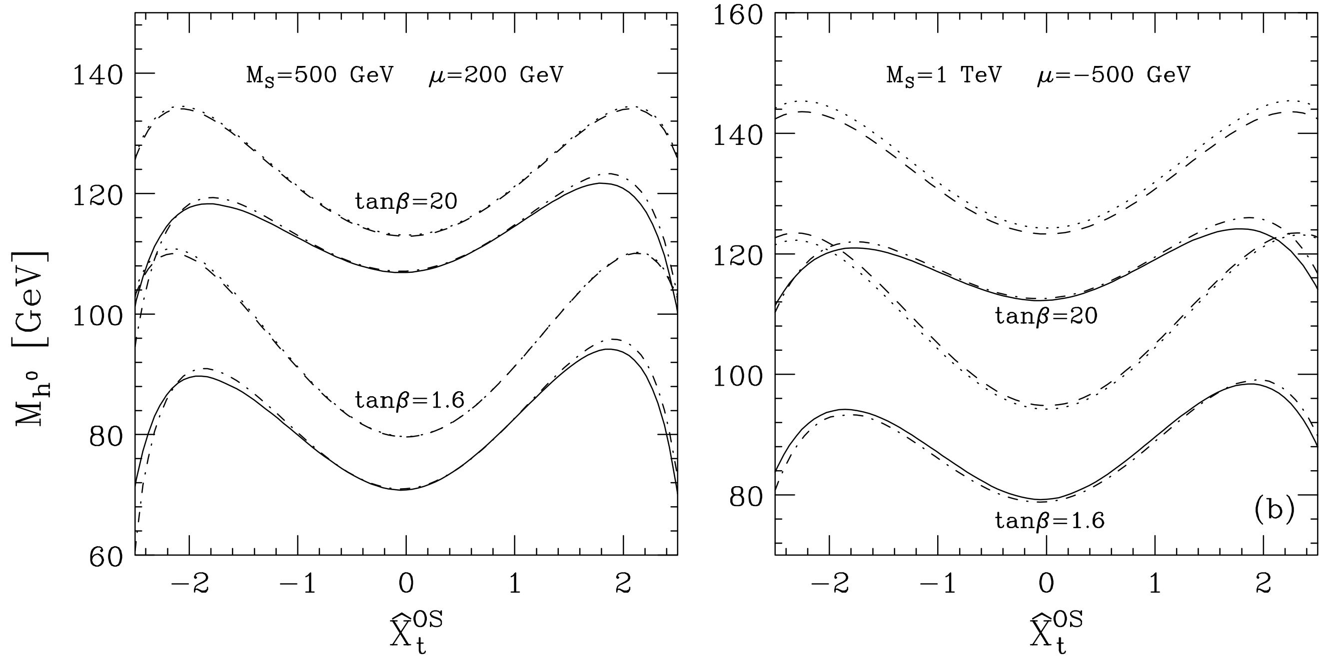

Figure 1: Higgs boson mass M_{h^0} vs. the on-shell top-squark mixing parameter $\hat{X}_t^{\rm OS}$. Dotted, dot-dashed lines show one-loop and two-loop $\mathcal{O}(\alpha_s\alpha_t)$ results from the program `FeynHiggs`, corresponding results from our numerical analyses are shown in dashed and solid lines respectively.

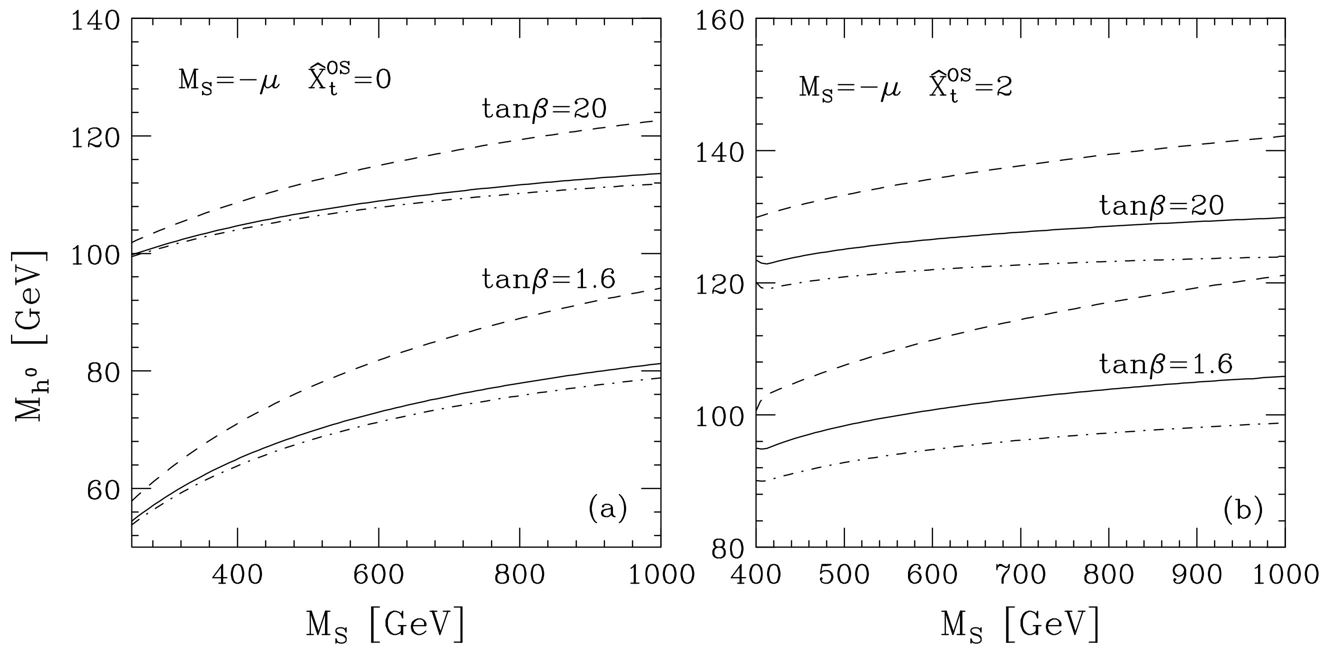

Figure 2: Higgs boson mass M_{h^0} vs. the on-shell SUSY scale M_S, for two top-squark mixing parameters $\hat{X}_t^{\rm OS} = 0$ and 2. One-loop mass, two-loop masses to $\mathcal{O}(\alpha_s\alpha_t)$ and $\mathcal{O}(\alpha_s\alpha_t + \alpha_t^2)$ are shown in dashed, dot-dashed and solid lines respectively.

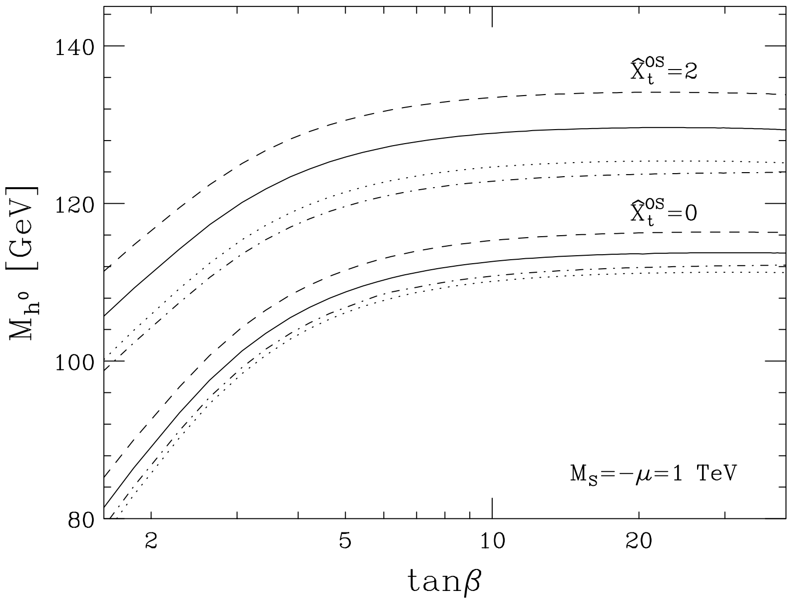

Figure 3: Higgs boson mass M_{h^0} vs. $\tan\beta$ for the top-squark mixing parameters $\hat{X}_t^{\rm OS} = 0$ and 2. Dot-dashed and solid lines correspond to two-loop Higgs boson masses to $\mathcal{O}(\alpha_s\alpha_t)$ and $\mathcal{O}(\alpha_s\alpha_t+\alpha_t^2)$ respectively for $M_t = 175$ GeV. Two-loop masses to $\mathcal{O}(\alpha_s\alpha_t + \alpha_t^2)$ for $M_t = 170$ and 180 GeV are also shown in dotted and dashed lines.

could contribute to (4) at the same order as $\Delta\mathcal{M}^2_{ij}$. It is not possible to obtain these self-energies in our current approach, and explicit two-loop calculation of the corresponding two-point functions are needed. Fortunately, the correction to m_{h^0} from Π_{AA} is always numerically negligible for large m_{A^0} as can be easily seen from the structure of the Higgs mass matrix (3). That is, (9) is correct for large m_{A^0} and we can safely neglect the Π_{AA} corrections. (For $m_{A^0} \sim m_Z$, a complete two-loop calculation of m_{h^0} would need Π_{AA}.)

Fig. 1 is used as calibration: we compare in it our numerical results for M_{h^0} including only up to two-loop $\mathcal{O}(\alpha_s\alpha_t)$ corrections with the mass obtained by the program `FeynHiggs` [17] which uses the explicit two-loop diagrammatic results of Ref. [9]. We choose two sets of parameters: (a) $M_{A^0} = M_3 = M^{\rm OS}_{\widetilde{Q}} = M^{\rm OS}_{\widetilde{U}} = M_S = 500$ GeV, $\mu = 200$ GeV and (b) $M_{A^0} = M_3 = M^{\rm OS}_{\widetilde{Q}} = M^{\rm OS}_{\widetilde{U}} = M_S = 1$ TeV, $\mu = -500$ GeV. For each case, results for two values of $\tan\beta$ (1.6 and 20) are plotted. We find good agreement (given the fact that they are two independent programs) between both one-loop (shown in dotted and dashed lines) and two-loop QCD corrected (shown in dot-dashed and solid lines) masses; this shows numerically that the two approaches are equivalent to that order. This equivalence is easily understood since the effective potential, as a generating functional [18], encompasses all tadpole and self-energy diagrams (as well as all other multi-point functions) which are calculated in [9]. The effective potential approach is more efficient for the purpose of calculating M_{h^0} and much simpler to implement in a `Fortran` program since it requires evaluating only one set of two-loop functions.

In Fig. 2 we show the Higgs boson mass M_{h^0} vs. the (on-shell) SUSY scale M_S, for two values of the top-squark mixing parameters $\hat{X}_t^{\rm OS}$ (0 and 2). All the physical masses M_{A^0}, $M^{\rm OS}_{\widetilde{Q}}$, $M^{\rm OS}_{\widetilde{U}}$ and M_3 have been set to M_S (and the same will be done for all the following plots). The dashed,

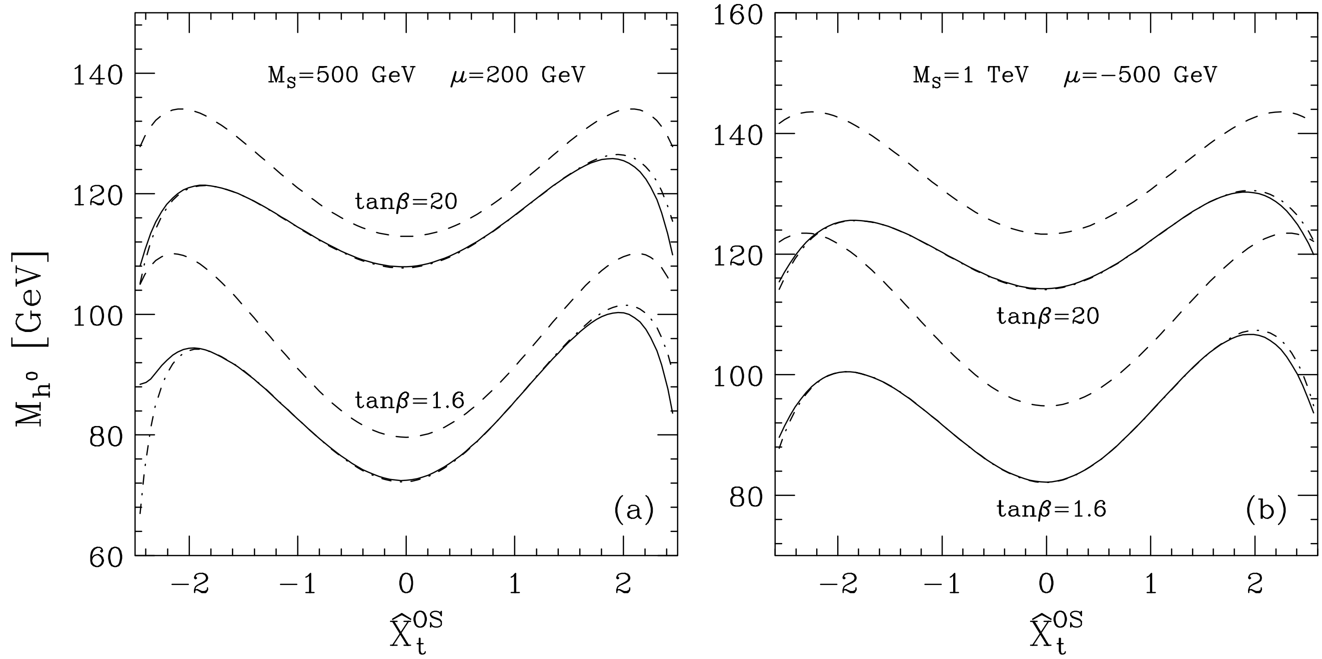

Figure 4: Higgs boson masses M_{h^0} vs. $\hat{X}_t^{\rm OS}$. One-loop masses, two-loop masses to $\mathcal{O}(\alpha_s\alpha_t + \alpha_t^2)$ and their approximations are shown in dashed, solid and dot-dashed lines.

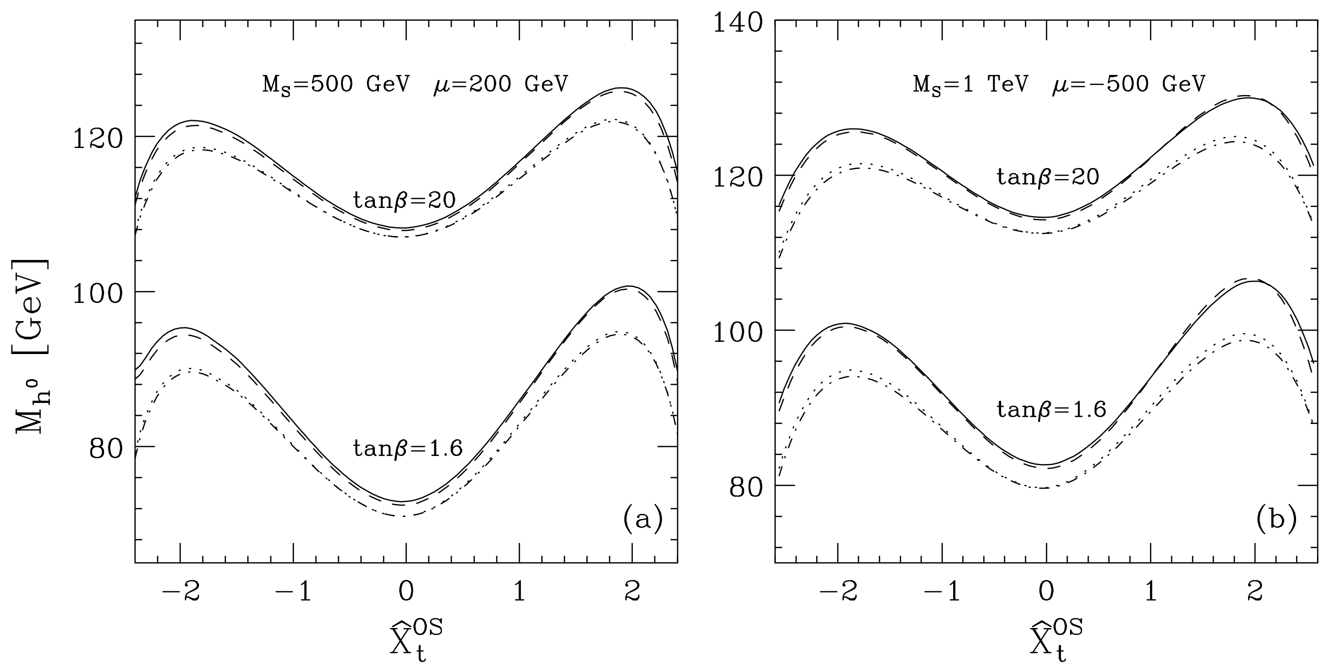

Figure 5: Higgs boson masses M_{h^0} vs. $\hat{X}_t^{\rm OS}$. Two-loop masses to $\mathcal{O}(\alpha_s\alpha_t)$ and $\mathcal{O}(\alpha_s\alpha_t + \alpha_t^2)$ are shown in dotted and dashed lines, their corresponding RG-corrected masses are shown in dot-dashed and solid lines.

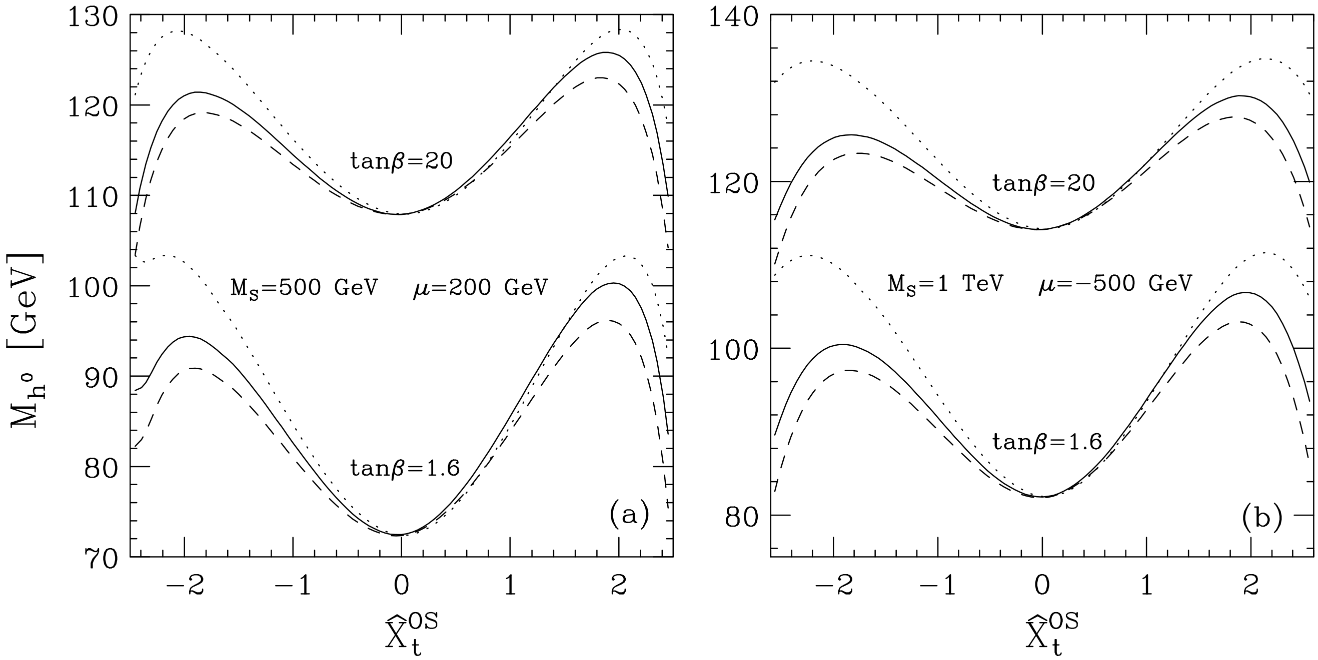

Figure 6: Higgs boson masses M_{h^0} vs. $\hat{X}_t^{\rm OS}$. Two-loop masses without the top-squark-mixing-dependent correction terms of Eq. (20) are shown in dotted lines. The corresponding masses without the $\mathcal{O}(\alpha_t^2)$ corrections only and the full numerical results are shown in dashed and solid lines respectively.

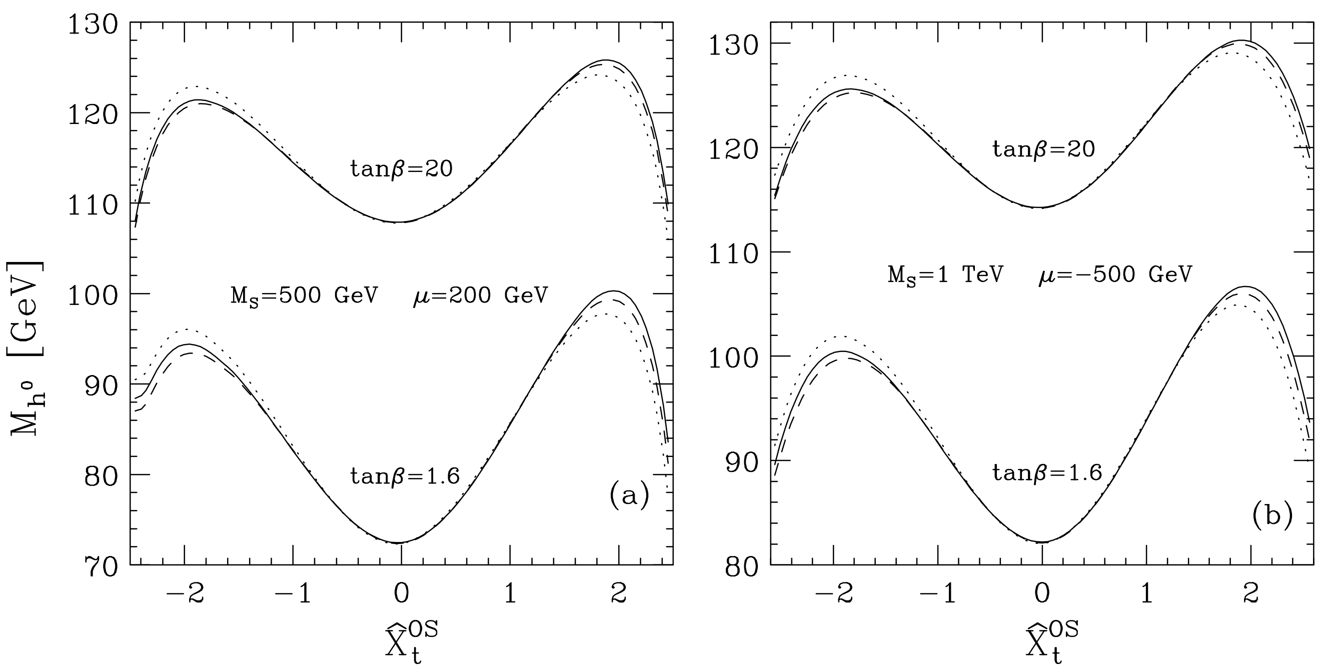

Figure 7: Higgs boson masses M_{h^0} vs. $\hat{X}_t^{\rm OS}$. Two-loop masses without the threshold correction term $\Delta_{\rm th}^{(2)} m_{h^0}^2$ are shown in dotted lines. The corresponding masses without the $\mathcal{O}(\alpha_t^2)$ threshold corrections only and with the full numerical results are shown in dashed and solid lines respectively.

dot-dashed and solid lines in this figure correspond to masses M_{h^0} corrected to one-loop, two-loop $\mathcal{O}(\alpha_s\alpha_t)$ and two-loop $\mathcal{O}(\alpha_s\alpha_t+\alpha_t^2)$ order[§]. Fig. 2a ($\hat{X}_t^{\rm OS}=0$) corresponds to the case of minimal left-right top-squark mixing, and the two-loop $\mathcal{O}(\alpha_t^2)$ corrections are generally small, $\lesssim 2$ GeV. For Fig. 2b ($\hat{X}_t^{\rm OS}=2$), which roughly corresponds to the maximal left-right top-squark mixing case, we find that the two-loop $\mathcal{O}(\alpha_t^2)$ corrections are sizable ($\simeq 5$ GeV).

In Fig. 3 we examine the upper limit on the Higgs boson mass M_{h^0} by including the dominant two-loop corrections. We show corrected massed to the two-loop $\mathcal{O}(\alpha_s\alpha_t)$ and $\mathcal{O}(\alpha_s\alpha_t+\alpha_t^2)$ orders in dot-dashed and solid lines for $\hat{X}_t^{\rm OS}=0,2$ and the top quark pole mass $M_t=175$ GeV. We see that maximal values for M_{h^0} of $\simeq 129$ GeV can be reached for large $\tan\beta$ and left-right top-squark mixing parameter $\hat{X}_t^{\rm OS}\simeq 2$. Without two-loop $\mathcal{O}(\alpha_t^2)$ corrections, the upper bound of M_{h^0} would be at $\simeq 124$ GeV. We also show the Higgs boson masses for $M_t=180$ and 170 GeV (including all two-loop dominant corrections) in dashed and dot-dashed lines; the masses are increased or decreased by ~ 5 GeV respectively. We remark that this upper bound on M_{h^0} is asymmetric with respect to $\hat{X}_t^{\rm OS}$. For $\hat{X}_t^{\rm OS}=-2$ and $M_t=175$ GeV, we find the bound is about 5 GeV lower. As is well know, this asymmetry arises from the two-loop $\mathcal{O}(\alpha_s\alpha_t)$ corrections [9, 6].

In Fig. 4 we compare results from our analytical approximation formula for M_{h^0} in Sec. 2 with those obtained by full numerical evaluations. They are shown in dot-dashed and solid lines respectively. The analytical approximation formula works remarkably well: it is good to a precision of $\lesssim 0.5$ GeV for almost all the parameter space. The analytical approximation has a complicated dependence on the μ-parameter. Numerically this dependence is quite weak: varying μ from 100 GeV to 1 TeV for a fixed $\hat{X}_t^{\rm OS}$ changes the Higgs boson mass by less than 1 GeV. We emphasize that the analytical formula is useful for several reasons: (1) the logarithmic and finite corrections can be easily separated, and one can weight the relative importance of these terms; (2) all terms can be traced back to the potential, so one can easily locate the particles giving the biggest contributions; (3) the formula can significantly simplify the numerical evaluations of M_{h^0} to a good precision.

In Fig. 5 we further compare the results for our RG-corrected Higgs boson masses, Eqs. (28-30), with those of the full numerical evaluation. For comparison, we have also shown two-loop $\mathcal{O}(\alpha_s\alpha_t)$ corrections and their RG-corrected results; they have been studied previously in [7]. As mentioned in Sect. 3, the good agreement between these curves is an indication of the smallness of the logarithmic corrections beyond two-loops and illustrates the accuracy of our results.

Finally in Figs. 6 and 7 we detail the size of the two-loop top-squark-mixing-dependent corrections in the OS-scheme and their corresponding finite threshold corrections in the RG approach. Fig. 6 shows in dotted lines two-loop masses without including the top-squark-mixing-dependent corrections of Eq. (20). Refs. [9, 6, 7] have already calculated the QCD corrections, and they are depicted in dashed lines. The difference of the solid and dashed lines is the two-loop $\mathcal{O}(\alpha_t^2)$ terms which are calculated in this paper. We see clearly that these terms are sizable: for large mixing parameters, they increase M_{h^0} by about 4 GeV and $2-3$ GeV for small and large $\tan\beta$ respectively.

Fig. 7 shows the effect of two-loop threshold corrections $\Delta_{\rm th}^{(2)}m_{h^0}^2$ evaluated following the RG-inspired analysis of Sect. 3. The dotted lines show the Higgs boson mass neglecting these corrections; this would have been obtained by integrating two-loop RG equations (with the two-loop boundary threshold correction being set to zero), as we have shown in the second part of Sec. 3.

[§]In general, we try to follow the rule that denser lines correspond to more precise approximations.

Two-loop masses without the $\mathcal{O}(\alpha_t^2)$ threshold correction and the complete two-loop results are shown in dashed and solid lines respectively. The RG reshuffling of radiative corrections has absorbed the main part of the two-loop top-squark-mixing-dependent terms of Eq. (20) into the RG-corrected one-loop term $\Delta_{\rm th}^{(1)} m_{h^0}^2$; the remaining genuine two-loop threshold corrections (in the sense of the effective field theory) are generally small, $\lesssim 3$ GeV.

5 Conclusions

In this paper we calculate radiative corrections to the lightest MSSM $\mathcal{CP}$-even Higgs boson mass to the two-loop $\mathcal{O}(\alpha_t^2)$ order. Our analysis extends existing two-loop diagrammatic results [5, 9, 6, 7] using a simpler effective potential approach and provides the most complete and accurate calculation presented in the literature. We also derive useful analytical approximation formulae, applicable when the supersymmetric particles are heavy, which accurately reproduce results from the full numerical study.

Our calculation includes effects which can have an impact on the final Higgs mass but were neglected by previous studies. In particular, the two-loop $\mathcal{O}(\alpha_t^2)$ top-squark-mixing-dependent corrections to $M_{h^0}^2$ [see Eq. (20)] are calculated for the first term in this paper and are numerically important.

We further simplify our analytical formula by reshuffling higher order logarithmic corrections (using RG techniques) in a compact one-loop expression [Eq. (28)]. In that expression all mass parameters are evaluated at appropriate renormalization scales chosen to reproduce the numerically most important leading and next-to-leading logarithmic corrections. The remaining two-loop finite terms can be interpreted as threshold corrections, and are numerically less important. This RG rewriting clarifies the structure of the two-loop corrections to $M_{h^0}^2$, identifies the most important contributions and links our work to the effective theory or RG approach, as we have shown in detail in Sec. 3.

To summarize our numerical results, we have shown that two-loop top Yukawa corrections to M_{h^0} are sizable for the maximal top-squark mixing case. They can increase the Higgs boson mass M_{h^0} by as much as 5 GeV (among which the top-squark-mixing-dependent corrections account for about 4 GeV) for small $\tan\beta$ where h_t is large. The upper bound on M_{h^0} is 129 ± 5 GeV for $M_t = 175 \pm 5$ GeV. Our final approximation formulae (20-21) and (28-30) have been shown to excellently agree with the full numerical results and can be easily implemented in precision numerical studies.

Although we have focussed in this paper on the Higgs mass, it is worth mentioning that we have also presented in Appendix D the MSSM two-loop effective potential including top-quark Yukawa contributions (for general top-squark mixing parameters and any $\tan\beta$). This knowledge may well prove useful for other studies.

Acknowledgments

We thank André Hoang for correspondence. R.-J.Z. was supported in part by a DOE grant No. DE-FG02-95ER40896 and in part by the Wisconsin Alumni Research Foundation.

Appendix A: One- and two-loop scalar functions

A.1 One-loop scalar functions

In this subsection we define the scalar functions A_0, B_0, B_1, B_{22} and G, which appear in one-loop self-energy calculations.

The A_0 function is defined by the following momentum integral in $d = 4 - 2\epsilon$ dimensions

$$A_0(m^2) \;=\; 16\pi^2\mu^{4-d}\int \frac{d^dp}{i(2\pi)^d}\frac{1}{p^2-m^2+i\varepsilon} \;=\; m^2\Big(\frac{1}{\epsilon}+1-\ln\frac{m^2}{Q^2}\Big)\ , \tag{A.1}$$

where $Q^2 = 4\pi\mu^2 e^{-\gamma_E}$ is the renormalization scale, with γ_E the Euler constant.

The B_0 function is

$$\begin{aligned} B_0(p^2,m_1^2,m_2^2) &= 16\pi^2\mu^{4-d}\int \frac{d^dq}{i(2\pi)^d}\frac{1}{[q^2-m_1^2+i\varepsilon][(q-p)^2-m_2^2+i\varepsilon]} \\ &= \frac{1}{\epsilon} - \int_0^1 dx\ \ln\frac{(1-x)m_1^2+xm_2^2-x(1-x)p^2-i\varepsilon}{Q^2}\ . \end{aligned} \tag{A.2}$$

The remaining functions can be related to A_0 and B_0 as follows

$$B_1(p^2,m_1^2,m_2^2) \;=\; \frac{1}{2p^2}\Big[A_0(m_2^2)-A_0(m_1^2)+(p^2+m_1^2-m_2^2)B_0(p^2,m_1^2,m_2^2)\Big]\ , \tag{A.3}$$

$$\begin{aligned} B_{22}(p^2,m_1^2,m_2^2) &= \frac{1}{6}\Big[A_0(m_2^2)+2m_1^2B_0(p^2,m_1^2,m_2^2)-(p^2+m_1^2-m_2^2)B_1(p^2,m_1^2,m_2^2) \\ &\qquad +m_1^2+m_2^2-\frac{p^2}{3}\Big]\ , \end{aligned} \tag{A.4}$$

$$G(p^2,m_1^2,m_2^2) \;=\; (p^2-m_1^2-m_2^2)B_0(p^2,m_1^2,m_2^2)-A_0(m_1^2)-A_0(m_2^2)\ . \tag{A.5}$$

In all one-loop expressions of radiative corrections, we adopt a (modified) minimal subtraction procedure to remove poles in ϵ and keep only finite (real) parts of the above functions.

Some useful expressions for these functions in limiting cases are (after minimal subtraction)

$$B_0(0,m_1^2,m_2^2) \;=\; 1-\ln\frac{m_1^2}{Q^2}+\frac{m_2^2}{m_1^2-m_2^2}\ln\frac{m_2^2}{m_1^2}\ , \tag{A.6}$$

$$B_0(m_1^2,m_2^2,0) \;=\; 2-\ln\frac{m_1^2}{Q^2}-\left(1-\frac{m_2^2}{m_1^2}\right)\ln\left(1-\frac{m_2^2}{m_1^2}\right)-\frac{m_2^2}{m_1^2}\ln\frac{m_2^2}{m_1^2}\ , \tag{A.7}$$

$$\frac{d}{dp^2}B_0(p^2,m^2,m^2)\bigg|_{p^2=0} \;=\; \frac{1}{6m^2}\ , \tag{A.8}$$

$$B_0(m^2,m^2,m^2) \;=\; -\ln\frac{m^2}{Q^2}+2-\frac{\pi}{\sqrt{3}}\ . \tag{A.9}$$

A.2 Two-loop scalar functions

In this subsection we collect some useful formulae of zero-point two-loop scalar functions. They have been studied extensively by several groups using two different methods: a differential equation method [19, 20] and an integral Mellin-Barnes transformation method [21]; their results all agree. Here we mainly follow Ref. [19].

The momentum integrals appearing in a two-loop effective potential calculation can be reduced to the following two types of scalar functions [corresponding to the topologies of two distinct zero-point two-loop irreducible Feynman diagrams (the figure-8 and sunset diagrams)]:

$$J(m_1^2, m_2^2) \;=\; -(16\pi^2\mu^{4-d})^2 \int \frac{d^dp\; d^dq}{(2\pi)^{2d}} \frac{1}{[p^2 - m_1^2 + i\varepsilon][q^2 - m_2^2 + i\varepsilon]} \;, \tag{A.10}$$

and

$$I(m_1^2, m_2^2, m_3^2) \;=\; (16\pi^2\mu^{4-d})^2 \int \frac{d^dp\; d^dq}{(2\pi)^{2d}} \frac{1}{[p^2 - m_1^2 + i\varepsilon][q^2 - m_2^2 + i\varepsilon][(p+q)^2 - m_3^2 + i\varepsilon]} \;. \tag{A.11}$$

The function J is symmetric in m_1, m_2 and I symmetric in m_1, m_2 and m_3.

The function J can be reduced to the product of one-loop scalar functions as

$$J(m_1^2, m_2^2) \;=\; A_0(m_1^2) A_0(m_2^2) \;. \tag{A.12}$$

The function I satisfies the following first-order partial differential equation [20]

$$\begin{aligned} R^2 \; \frac{\partial}{\partial m_3^2} I(m_1^2, m_2^2, m_3^2) \;&=\; (d-3)(m_3^2 - m_1^2 - m_2^2) I(m_1^2, m_2^2, m_3^2) \\ +\;\; (d-2)\Big[&\frac{m_3^2 - m_1^2 + m_2^2}{2m_3^2} J(m_1^2, m_3^2) + \frac{m_3^2 + m_1^2 - m_2^2}{2m_3^2} J(m_2^2, m_3^2) - J(m_1^2, m_2^2)\Big] \;, \end{aligned} \tag{A.13}$$

where

$$R^2 \;=\; m_1^4 + m_2^4 + m_3^4 - 2m_1^2 m_2^2 - 2m_1^2 m_3^2 - 2m_2^2 m_3^2 \;. \tag{A.14}$$

This differential equation can be used to solve for the I function. The initial value of this function can be evaluated from (A.13) which reduces to a simple algebraic equation when $m_3 = m_1 + m_2$, *i.e.* $R = 0$.

In our calculation, any Feynman diagram in the two-loop effective potential is subtracted by all its possible one-loop sub-diagrams; this is done by replacing the I and J functions as follows [19]:

$$\begin{aligned} I(m_1^2, m_2^2, m_3^2) \;&\to\; \hat{I}(m_1^2, m_2^2, m_3^2) = I(m_1^2, m_2^2, m_3^2) - \frac{1}{\epsilon}\Big[A_0(m_1^2) + A_0(m_2^2) + A_0(m_3^2)\Big] \;, \\ J(m_1^2, m_2^2) \;&\to\; \hat{J}(m_1^2, m_2^2) = J(m_1^2, m_2^2) + \frac{1}{\epsilon}\Big[m_1^2 A_0(m_2^2) + m_2^2 A_0(m_1^2)\Big] \;. \end{aligned} \tag{A.15}$$

It is then straightforward to show

$$\hat{J}(m_1^2, m_2^2) \;=\; -\frac{m_1^2 m_2^2}{\epsilon^2} + m_1^2 m_2^2 \Big(1 - \ln\frac{m_1^2}{Q^2}\Big)\Big(1 - \ln\frac{m_2^2}{Q^2}\Big) \;, \tag{A.16}$$

and with some effort

$$\hat{I}(m_1^2, m_2^2, m_3^2) \;=\; \frac{1}{2\epsilon^2}(m_1^2 + m_2^2 + m_3^2) - \frac{1}{2\epsilon}(m_1^2 + m_2^2 + m_3^2)$$

$$
\begin{aligned}
&- \frac{1}{2}\Big[(-m_1^2+m_2^2+m_3^2)\ln\frac{m_2^2}{Q^2}\ln\frac{m_3^2}{Q^2}+(m_1^2-m_2^2+m_3^2)\ln\frac{m_1^2}{Q^2}\ln\frac{m_3^2}{Q^2} \\
&+ (m_1^2+m_2^2-m_3^2)\ln\frac{m_1^2}{Q^2}\ln\frac{m_2^2}{Q^2}-4\Big(m_1^2\ln\frac{m_1^2}{Q^2}+m_2^2\ln\frac{m_2^2}{Q^2}+m_3^2\ln\frac{m_3^2}{Q^2}\Big) \\
&+ \xi(m_1^2,m_2^2,m_3^2)+5(m_1^2+m_2^2+m_3^2)\Big]\,, \qquad (A.17)
\end{aligned}
$$

where (for $R^2 > 0$) ξ is given by [21]

$$
\begin{aligned}
\xi(m_1^2,m_2^2,m_3^2) &= R\Big[2\ln\Big(\frac{m_3^2+m_1^2-m_2^2-R}{2m_3^2}\Big)\ln\Big(\frac{m_3^2-m_1^2+m_2^2-R}{2m_3^2}\Big)-\ln\frac{m_1^2}{m_3^2}\ln\frac{m_2^2}{m_3^2} \\
&- 2Li_2\Big(\frac{m_3^2+m_1^2-m_2^2-R}{2m_3^2}\Big)-2Li_2\Big(\frac{m_3^2-m_1^2+m_2^2-R}{2m_3^2}\Big)+\frac{\pi^2}{3}\Big]\,, \qquad (A.18)
\end{aligned}
$$

where $Li_2(x)$ is the dilogarithm function

$$
Li_2(x) = -\int_0^1 dy\,\frac{\ln(1-xy)}{y}\,. \qquad (A.19)
$$

In the region where $R^2 < 0$, (A.18) should be replaced by its analytical continuation. Equivalent expressions for ξ also appear in [19] and [20]; we find that (A.18) is most convenient for series expansions. We also define a function L for future use

$$
L(m_1^2,m_2^2,m_3^2) = J(m_2^2,m_3^2)-J(m_1^2,m_2^2)-J(m_1^2,m_3^2)-(m_1^2-m_2^2-m_3^2)I(m_1^2,m_2^2,m_3^2)\,. \qquad (A.20)
$$

Performing a (modified) minimal subtraction (by removing the single and double poles in ϵ), it is the finite (real) parts of (A.16) and (A.17) that we use in our two-loop effective potential expressions. We will also omit the carets of $\hat{I}$ and $\hat{J}$ to simplify the notation.

When computing the two-loop potential, some argument of the I function, *e.g.* the bottom-quark mass m_b, tree-level Higgs boson mass m_{h^0}, can be taken to be zero. The function I is well-behaved in these limiting cases:

$$
\begin{aligned}
I(m_1^2,m_2^2,0) &= -m_1^2\ln\frac{m_1^2}{Q^2}\ln\frac{m_2^2}{Q^2}-(m_1^2-m_2^2)\ln\frac{m_1^2-m_2^2}{Q^2}\ln\frac{m_1^2}{m_2^2}+\frac{1}{2}(m_1^2-m_2^2)\ln^2\frac{m_1^2}{Q^2} \\
&+ 2\Big(m_1^2\ln\frac{m_1^2}{Q^2}+m_2^2\ln\frac{m_2^2}{Q^2}\Big)-\frac{5}{2}(m_1^2+m_2^2)+(m_1^2-m_2^2)\Big[-\frac{\pi^2}{6}+Li_2\left(\frac{m_2^2}{m_1^2}\right)\Big]\,, \qquad (A.21) \\
I(m^2,0,0) &= -m^2\Big(\frac{1}{2}\ln^2\frac{m^2}{Q^2}-2\ln\frac{m^2}{Q^2}+\frac{5}{2}+\frac{\pi^2}{6}\Big)\,, \qquad (A.22)
\end{aligned}
$$

where we have kept only the finite terms as explained before. In (A.21) we have implicitly assumed $m_1 \geq m_2$. The symmetry of the above expression for $I(m_1^2, m_2^2, 0)$ in m_1 and m_2 [which obviously follows from the definition (A.15) of I] can be explicitly checked by using the identity

$$
Li_2(x) = -Li_2(x^{-1})-\frac{1}{2}\ln^2(-x)-\frac{\pi^2}{6}\,. \qquad (A.23)
$$

Finally, we collect expansion formulae for the function ξ which we use in the derivation of an analytical approximation formula for the two-loop Higgs boson mass corrections. The ξ functions we find can be reduced to one of the different types we list below using the relation

$$\xi(m_1^2, m_2^2, m_3^2) \;=\; m_1^2 \xi(1, m_2^2/m_1^2, m_3^2/m_1^2) \;. \tag{A.24}$$

(1) For $0 \le r \le 1$ and $0 \le \epsilon \ll 1$:

$$\begin{aligned}
\xi(1,r,\epsilon) \;&=\; (1-r)\left\{\frac{\pi^2}{3} + \Big[\ln\epsilon - 2\ln(1-r)\Big]\ln r - 2Li_2(r)\right\} \\
&-\; \epsilon\left\{2 - 2\ln\epsilon + \ln r + \frac{1+r}{1-r}\left[\frac{\pi^2}{3} + \Big(\ln\epsilon - 2\ln(1-r) - 1\Big)\ln r - 2Li_2(r)\right]\right\} \\
&+\; \frac{\epsilon^2}{(1-r)^3}\left\{\left(\frac{3}{2} - \ln\epsilon\right)(1-r^2) - \frac{2\pi^2}{3}r - \Big[2\ln\epsilon + r - 4\ln(1-r)\Big]r\ln r \right. \\
&\qquad \left. + 4r Li_2(r)\right\} + \mathcal{O}(\epsilon^3) \;.
\end{aligned} \tag{A.25}$$

If $r > 1$, one uses $\xi(1,r,\epsilon) = r\xi(1,1/r,\epsilon/r)$ and the above expression.

Two particular cases of the previous expansion are:

(1a) For $0 \le \epsilon_1, \epsilon_2 \ll 1$:

$$\begin{aligned}
\xi(1,\epsilon_1,\epsilon_2) \;&=\; \frac{\pi^2}{3} + \ln\epsilon_1\ln\epsilon_2 - 2\Big(-1 + \frac{\pi^2}{3} + \ln\epsilon_1\ln\epsilon_2\Big)\epsilon_1\epsilon_2 \\
&+\; \left[\Big(-2 - \frac{\pi^2}{3} + 2\ln\epsilon_1 - \ln\epsilon_1\ln\epsilon_2\Big)\epsilon_1 + \Big(\frac{3}{2} - \ln\epsilon_1\Big)\epsilon_1^2 + (\epsilon_1 \leftrightarrow \epsilon_2)\right] + \mathcal{O}(\epsilon_1^m\epsilon_2^n) \;,
\end{aligned} \tag{A.26}$$

with $m + n = 3$, and

(1b) For $0 \le |\epsilon_1|, \epsilon_2 \ll 1$:

$$\begin{aligned}
\xi(1,1+\epsilon_1,\epsilon_2) \;&=\; -2(4 + \epsilon_1 - 2\ln\epsilon_2)\epsilon_2 + \Big(\frac{8}{9} - \frac{1}{3}\ln\epsilon_2\Big)\epsilon_2^2 \\
&+\; \left[2 - \ln\epsilon_2 + \Big(\frac{7}{18} + \frac{1}{6}\ln\epsilon_2\Big)\epsilon_2\right]\epsilon_1^2 \\
&+\; \Big(-\frac{1}{2} + \frac{1}{2}\ln\epsilon_2\Big)\epsilon_1^3 + \Big(\frac{2}{9} - \frac{1}{3}\ln\epsilon_2\Big)\epsilon_1^4 + \mathcal{O}(\epsilon_1^m\epsilon_2^n) \;,
\end{aligned} \tag{A.27}$$

with $m + 2n \ge 5$.

Finally we also give

(2) For $|\epsilon_1|, |\epsilon_2| \ll 1$:

$$\begin{aligned}
\xi(1,1+\epsilon_1,1+\epsilon_2) \;&=\; 36K + (8K-1)\epsilon_1\epsilon_2 + \Big(\frac{5}{36} - \frac{8}{3}K\Big)\epsilon_1^2\epsilon_2^2 \\
&+\; \left\{12K\epsilon_1 + (1-8K)\epsilon_1^2 + \Big(\frac{8}{3}K - \frac{2}{9}\Big)\epsilon_1^3 + \Big(\frac{1}{108} - \frac{16}{9}K\Big)\epsilon_1^4 \right. \\
&+\; \left. \left[-\frac{\epsilon_1^2}{6} + \Big(\frac{11}{54} + \frac{8}{9}K\Big)\epsilon_1^3\right]\epsilon_2 + (\epsilon_1 \leftrightarrow \epsilon_2)\right\} + \mathcal{O}(\epsilon_1^m\epsilon_2^n) \;,
\end{aligned} \tag{A.28}$$

with $m + n = 5$. In this expansion the constant number K is given by

$$K \;=\; -\frac{1}{\sqrt{3}}\int_0^{\pi/6} dx \;\ln(2\cos x) \simeq -0.1953256 \;. \tag{A.29}$$

Appendix B: MSSM in the leading approximation

The general structure of the MSSM is quite complicated, with many different fields and field mixings. This makes the computation of the complete potential prohibitive at two-loops. However, it is a good aproximation to keep only those terms of the MSSM Lagrangian which depend of the $SU(3)$ gauge coupling g_3 and the top Yukawa h_t (and neglect the electroweak gauge couplings g_1, g_2 and the rest of the Yukawa couplings). We call this the leading approximation and it greatly simplifies our two-loop effective potential calculation. In this Appendix, we summarize the necessary Feynman rules for computing the two-loop potential in this leading approximation and also some MSSM renormalization group equations, useful to check the scale invariance of the potential.

B.1 Masses and Feynman rules

The Higgs sector scalar potential in the leading approximation is

$$V_{\text{Higgs}} = (m_{H_1}^2 + \mu^2)|H_1|^2 + (m_{H_2}^2 + \mu^2)|H_2|^2 + B_\mu(H_1 H_2 + \text{H.c.}) \ , \tag{B.1}$$

where m_{H_1}, m_{H_2} and B_μ [with dimensions of (mass)^2] are the soft-breaking Higgs mass parameters, and μ the supersymmetric Higgs-boson mass parameter. Although we do not write the quartic Higgs couplings, which depend on the electroweak gauge coupling constants, they are responsible for the tree-level mass of the lightest Higgs boson, which we of course include in our calculations.

The $SU(2)$ doublet Higgs fields H_1 and H_2 can be written as follows:

$$H_1 = \left[\begin{array}{c} (h_1 + i a_1)/\sqrt{2} \\ h_1^- \end{array} \right] , \qquad H_2 = \left[\begin{array}{c} h_2^+ \\ (h_2 + i a_2)/\sqrt{2} \end{array} \right] . \tag{B.2}$$

In our approximation, the mass-squared matrices for $\mathcal{CP}$-even and odd Higgs fields are

$$\mathcal{M}_\pm^2 = \left(\begin{array}{cc} m_{H_1}^2 + \mu^2 & \pm B_\mu \\ \pm B_\mu & m_{H_2}^2 + \mu^2 \end{array} \right) , \tag{B.3}$$

where the positive (negative) sign applies to the $\mathcal{CP}$-even (odd) fields respectively. The charged Higgs fields have the same mass-squared matrix $\mathcal{M}_-^2$ as the $\mathcal{CP}$-odd Higgses.

The $\mathcal{CP}$-even interaction eigenstates $h_1,\ h_2$ are rotated by the angle α into the mass eigenstates H^0 and h^0. Similarly, the $\mathcal{CP}$-odd states $a_1,\ a_2$ (charged states $h_1^+,\ h_2^+$) are rotated into mass eigenstates G^0 and A^0 (G^+ and H^+) by the angle β. This angle β is conventionally defined in terms of the $\mathcal{CP}$-even Higgs field VEVs, $\langle h_{1,2}\rangle = v_{1,2}$, by $\tan\beta = v_2/v_1$. The fact that β diagonalizes $\mathcal{M}_-^2$ is obvious when the minimization conditions of the potential (B.1), $m_{H_1}^2 + \mu^2 = -B_\mu \tan\beta$ and $m_{H_2}^2 + \mu^2 = -B_\mu \cot\beta$, are imposed and the soft parameters in the matrix are replaced by $\tan\beta$ and $m_{A^0}^2 = -B_\mu(\tan\beta + \cot\beta)$. Since we have neglected all $g_1,\ g_2$ related terms in (B.1), in our approximation (we use shorthand notations $c_\beta = \cos\beta,\ s_\beta = \sin\beta,\ etc.$)

$$c_\alpha = s_\beta, \quad \text{and } s_\alpha = -c_\beta \ . \tag{B.4}$$

This approximation is excellent when $M_{A^0} \gg M_Z$ but would fail for $M_{A^0} \sim M_Z$. The effect is numerically relevant for the tree level masses and we take it into account, but it may be consistently neglected in the two-loop corrections.

The (field-dependent) top squark mass-squared matrix in the leading approximation is

$$\mathcal{M}_{\tilde{t}}^2 \;=\; \left[\begin{array}{cc} M_{\widetilde{Q}}^2 + \frac{1}{2}h_t^2 h_2^2 & \frac{1}{\sqrt{2}}h_t(A_t h_2 + \mu h_1) \\ \frac{1}{\sqrt{2}}h_t(A_t h_2 + \mu h_1) & M_{\widetilde{U}}^2 + \frac{1}{2}h_t^2 h_2^2 \end{array}\right] , \tag{B.5}$$

where $M_{\widetilde{Q}}$, $M_{\widetilde{U}}$ are soft-breaking mass parameters of the left- and right-handed top-squarks $\widetilde{Q}$ and $\widetilde{U}$, and A_t the usual trilinear soft-breaking parameter. Denoting the mass eigenvalues of the matrix (B.5) by $m_{\tilde{t}_1}$, $m_{\tilde{t}_2}$ and the mixing angle by $\theta_{\tilde{t}}$, the Feynman rules for Higgs/Goldstone-boson-top squark trilinear coupling are simply $-i\lambda$, with λ as listed below:

$$\begin{aligned}
\lambda_{H^+\tilde{t}_1\tilde{b}_L} &= -h_t(c_t m_t + s_t Y_t)c_\beta \ , & \lambda_{H^+\tilde{t}_2\tilde{b}_L} &= h_t(s_t m_t - c_t Y_t)c_\beta \ , \\
\lambda_{G^+\tilde{t}_1\tilde{b}_L} &= -h_t(c_t m_t + s_t X_t)s_\beta \ , & \lambda_{G^+\tilde{t}_2\tilde{b}_L} &= -h_t(s_t m_t - c_t X_t)s_\beta \ , \\
\lambda_{H^0\tilde{t}_1\tilde{t}_1} &= -\sqrt{2}h_t(m_t + s_t c_t Y_t)c_\beta \ , & \lambda_{H^0\tilde{t}_2\tilde{t}_2} &= -\sqrt{2}h_t(m_t - s_t c_t Y_t)c_\beta \ , \\
\lambda_{h^0\tilde{t}_1\tilde{t}_1} &= \sqrt{2}h_t(m_t + s_t c_t X_t)s_\beta \ , & \lambda_{h^0\tilde{t}_2\tilde{t}_2} &= \sqrt{2}h_t(m_t - s_t c_t X_t)s_\beta \ , \\
\lambda_{H^0\tilde{t}_1\tilde{t}_2} &= -\frac{1}{\sqrt{2}}h_t c_{2t} Y_t c_\beta \ , & \lambda_{h^0\tilde{t}_1\tilde{t}_2} &= \frac{1}{\sqrt{2}}h_t c_{2t} X_t s_\beta \ , \\
\lambda_{A^0\tilde{t}_1\tilde{t}_2} = -\lambda_{A^0\tilde{t}_2\tilde{t}_1} &= \frac{1}{\sqrt{2}}h_t Y_t c_\beta \ , & \lambda_{G^0\tilde{t}_1\tilde{t}_2} = -\lambda_{G^0\tilde{t}_2\tilde{t}_1} &= \frac{1}{\sqrt{2}}h_t X_t s_\beta \ ,
\end{aligned} \tag{B.6}$$

where $c_t = \cos\theta_{\tilde{t}}$, $s_t = \sin\theta_{\tilde{t}}$, $c_{2t} = \cos 2\theta_{\tilde{t}}$ and

$$X_t \;=\; A_t + \mu\cot\beta, \qquad Y_t \;=\; A_t - \mu\tan\beta \ . \tag{B.7}$$

The couplings of squarks to neutralinos and charginos are very simple in the leading approximation, since the gaugino-Higgsino mixing can be neglected and the only interactions are Higgsino-squark interactions. The Feynman rules for the $\tilde{h}_i^0 t\tilde{t}_j$ couplings can be written as $-i(a\mathcal{P}_L + b\mathcal{P}_R)$ and that of $\tilde{h}^+ t\tilde{b}_L$ as $i\mathcal{C}^{-1}(a\mathcal{P}_L + b\mathcal{P}_R)$ ($\mathcal{P}_{L,R}$ are chiral projectors and $\mathcal{C}$ the charge-conjugation matrix), with

$$\begin{aligned}
&a_{\tilde{h}_1^0 t\tilde{t}_1} = -ia_{\tilde{h}_2^0 t\tilde{t}_1} = b_{\tilde{h}_1^0 t\tilde{t}_2} = ib_{\tilde{h}_2^0 t\tilde{t}_2} = \frac{h_t}{\sqrt{2}}c_t \ , \\
&-a_{\tilde{h}_1^0 t\tilde{t}_2} = ia_{\tilde{h}_2^0 t\tilde{t}_2} = b_{\tilde{h}_1^0 t\tilde{t}_1} = ib_{\tilde{h}_2^0 t\tilde{t}_1} = \frac{h_t}{\sqrt{2}}s_t \ , \\
&a_{\tilde{h}^+ t\tilde{b}_L} = -h_t \ , \qquad a_{\tilde{h}^+ b\tilde{t}_1} = -h_t s_t \ , \qquad a_{\tilde{h}^+ b\tilde{t}_2} = -h_t c_t \ ,
\end{aligned} \tag{B.8}$$

when $\mu > 0$; for $\mu < 0$, we only need to interchange $a_{\tilde{h}_1^0 t\tilde{t}_i}$ and $a_{\tilde{h}_2^0 t\tilde{t}_i}$, as well as $b_{\tilde{h}_1^0 t\tilde{t}_i}$ and $b_{\tilde{h}_2^0 t\tilde{t}_i}$.

Other Feynman rules of $\mathcal{O}(g_3)$ and $\mathcal{O}(h_t)$ vertices are exactly the same as in the general MSSM and we do not present them explicitly.

B.2 Renormalization group equations

The MSSM RGEs [23] that we will use to check the invariance of the potential to two-loop order under renormalization scale transformations are the following. First, we need the two-loop RGEs for those parameters entering in the tree-level potential (B.1)

$$\frac{\partial m_{H_2}^2}{\partial \ln Q^2} = \frac{3h_t^2}{16\pi^2}\mathcal{M}_t^2 + \frac{16g_3^2h_t^2}{(16\pi^2)^2}(\mathcal{M}_t^2 + 2M_3^2 - 2M_3A_t) - \frac{18h_t^4}{(16\pi^2)^2}(\mathcal{M}_t^2 + A_t^2) \ , \tag{B.9}$$

$$\frac{\partial \ln \mu}{\partial \ln Q^2} = -\frac{\partial \ln h_2}{\partial \ln Q^2} = \frac{3h_t^2}{32\pi^2} + \frac{8g_3^2h_t^2}{(16\pi^2)^2} - \frac{9}{2}\frac{h_t^4}{(16\pi^2)^2} \ , \tag{B.10}$$

$$\begin{aligned}\frac{\partial B_\mu}{\partial \ln Q^2} &= \frac{3h_t^2}{16\pi^2}\left(\frac{B_\mu}{2} + A_t\mu\right) + \frac{16g_3^2h_t^2}{(16\pi^2)^2}\left(\frac{B_\mu}{2} + A_t\mu - M_3\mu\right) \\ &- \frac{9h_t^4}{(16\pi^2)^2}\left(\frac{B_\mu}{2} + 2A_t\mu\right) \ ,\end{aligned} \tag{B.11}$$

where $\mathcal{M}_t^2 = m_{H_2}^2 + M_{\widetilde{Q}}^2 + M_{\widetilde{U}}^2 + A_t^2$. Then we need one-loop RGEs for those masses entering in the one-loop potential

$$16\pi^2\,\frac{\partial m_t^2}{\partial \ln Q^2} = \left(-\frac{16g_3^2}{3} + 3h_t^2\right)m_t^2 \ , \tag{B.12}$$

$$\begin{aligned}16\pi^2\,\frac{\partial m_{\tilde t_1}^2}{\partial \ln Q^2} &= -\frac{16g_3^2}{3}\left[m_t^2 + M_3^2 - s_{2t}m_t\left(M_3 - \frac{X_t}{2}\right)\right] \\ &+ h_t^2\left[3m_t^2 + (1+s_t^2)\mathcal{M}_t^2 + 3s_{2t}m_t\left(A_t + \frac{3X_t}{2}\right)\right] \ ,\end{aligned} \tag{B.13}$$

$$\begin{aligned}16\pi^2\,\frac{\partial m_{\tilde t_2}^2}{\partial \ln Q^2} &= -\frac{16g_3^2}{3}\left[m_t^2 + M_3^2 + s_{2t}m_t\left(M_3 - \frac{X_t}{2}\right)\right] \\ &+ h_t^2\left[3m_t^2 + (1+c_t^2)\mathcal{M}_t^2 - 3s_{2t}m_t\left(A_t + \frac{3X_t}{2}\right)\right] \ ,\end{aligned} \tag{B.14}$$

$$16\pi^2\,\frac{\partial m_{H_n^0}^2}{\partial \ln Q^2} = 3h_t^2\left[\mu^2 + D_n\mathcal{M}_t^2 + E_n\left(\frac{B_\mu}{2} + A_t\mu\right)\right] \ , \tag{B.15}$$

$$16\pi^2\,\frac{\partial m_{H_n^+}^2}{\partial \ln Q^2} = 3h_t^2\left[\mu^2 + D_{n+2}\mathcal{M}_t^2 + E_{n+2}\left(\frac{B_\mu}{2} + A_t\mu\right)\right] \ , \tag{B.16}$$

where $D_n = s_\alpha^2, c_\alpha^2, s_\beta^2, c_\beta^2$ and $E_n = s_{2\alpha}, -s_{2\alpha}, -s_{2\beta}, s_{2\beta}$ for $n = 1,2,3,4$. [Here we use the α angle to keep track the H^0 and h^0 contributions; it can be replaced by the β angle as in (B.4) in the leading approximation.] The ordering of the Higgs/Goldstone bosons are $H_n^0 = H^0, h^0, G^0$ and A^0 for $n = 1,2,3,4$ and $H_n^+ = G^+, H^+$ for $n = 1,2$. Eqs. (B.13-B.16) seem unfamiliar, but they follow directly from (B.3), (B.5) and the one-loop MSSM RGEs of soft parameters entering those equations.

Using (B.13) and (B.14), we find one-loop RGEs for X_t and $m_{\tilde t}^2$, the (arithmetic) average of the (squared) top squark masses. They are

$$16\pi^2\,\frac{\partial X_t}{\partial \ln Q^2} = \frac{16}{3}g_3^2M_3 + 3h_t^2(A_t + X_t) \ . \tag{B.17}$$

$$16\pi^2\,\frac{\partial m_{\tilde t}^2}{\partial \ln Q^2} = -\frac{16}{3}g_3^2(m_t^2 + M_3^2) + h_t^2\left(3m_t^2 + \frac{3}{2}\mathcal{M}_t^2\right) \ , \tag{B.18}$$

these two equations are used in Sec. 3 for the RG discussion of the formula for the Higgs boson mass M_{h^0}. Eq. (B.17) can also be derived from (B.7) and one-loop RGEs of A_t, μ and $\tan\beta$.

Appendix C: One-loop self-energies

In this appendix, we collect formulae for those MSSM one-loop self-energies which are necessary for our analysis. We present these self-energies in the leading approximation of keeping only h_t and g_3-dependent terms, as explained in Appendix B; their full form can be found in Ref. [10], which we follow for notation. (See also [24] for top quark/squark self-energies.)

–Top quark:

$$
\begin{aligned}
16\pi^2\ \Sigma_t(p^2) &= \frac{4g_3^2}{3}\Big\{m_t\Big[B_1(p^2,m_{\tilde g}^2,m_{\tilde t_1}^2)+B_1(p^2,m_{\tilde g}^2,m_{\tilde t_2}^2)\Big]-m_t\Big(5-3\ln\frac{m_t^2}{Q^2}\Big)\\
&- s_{2t}\ m_{\tilde g}\Big[B_0(p^2,m_{\tilde g}^2,m_{\tilde t_1}^2)-B_0(p^2,m_{\tilde g}^2,m_{\tilde t_2}^2)\Big]\Big\}\\
&+ \frac{h_t^2}{2}m_t\Big\{c_\beta^2\Big[2B_1(p^2,m_t^2,m_{A^0}^2)+B_1(p^2,m_b^2,m_{A^0}^2)\Big]\\
&+ s_\beta^2\Big[2B_1(p^2,m_t^2,m_Z^2)+B_1(p^2,m_b^2,m_Z^2)\Big]\\
&+ B_1(p^2,\mu^2,m_{\tilde t_1}^2)+B_1(p^2,\mu^2,m_{\tilde t_2}^2)+B_1(p^2,\mu^2,m_{\tilde b_L}^2)\Big\}\ ,
\end{aligned}
\tag{C.1}
$$

where we have assumed all heavy Higgs bosons have mass m_{A^0} much larger than the masses of the light Higgs and W-boson, taken to be $\sim m_Z$.

From (C.1) we find the running top-quark mass at the scale Q (under the simplified assumptions of a common heavy SUSY scale M_S while the μ parameter is left free, see Sec. 2)

$$
\begin{aligned}
m_t^2(Q) &= M_t^2\Big\{1-\frac{g_3^2}{6\pi^2}\Big[5-3\ln\frac{m_t^2}{Q^2}+\ln\frac{M_S^2}{Q^2}-\hat X_t\Big] \qquad \text{(C.2)}\\
&+ \frac{3h_t^2}{32\pi^2}\Big[(1+c_\beta^2)\Big(\frac{1}{2}-\ln\frac{M_S^2}{Q^2}\Big)+s_\beta^2\Big(\frac{8}{3}-\ln\frac{m_t^2}{Q^2}\Big)-\frac{\hat\mu^2}{1-\hat\mu^2}\Big(1+\frac{\hat\mu^2}{1-\hat\mu^2}\ln\hat\mu^2\Big)\Big]\Big\}\ .
\end{aligned}
$$

In this equation we have neglected the external momentum and used (A.3) and (A.6). We have used the reduced parameters $\hat X_t\equiv X_t/M_S$, $\hat\mu\equiv\mu/M_S$ and M_t is the top quark pole mass (we use capital letters to denote on-shell mass parameters).

–Top squarks:

$$
\begin{aligned}
16\pi^2\ \Pi_{\tilde t_L\tilde t_L}(p^2) &= \frac{8g_3^2}{3}\Big\{G(p^2,m_{\tilde g}^2,m_t^2)+c_t^2\Big[A_0(m_{\tilde t_1}^2)-(p^2+m_{\tilde t_1}^2)B_0(p^2,m_{\tilde t_1}^2,0)\Big]\\
&+ s_t^2\Big[A_0(m_{\tilde t_2}^2)-(p^2+m_{\tilde t_2}^2)B_0(p^2,m_{\tilde t_2}^2,0)\Big]\Big\}\\
&+ h_t^2\Big[s_t^2A_0(m_{\tilde t_1}^2)+c_t^2A_0(m_{\tilde t_2}^2)+\frac{1}{2}\sum_{n=1}^{4}D_nA_0(m_{H_n^0}^2)+G(p^2,\mu^2,m_t^2)\Big]\\
&+ \sum_{n=1}^{4}\sum_{i=1}^{2}\lambda^2_{H_n^0\tilde t_L\tilde t_i}B_0(p^2,m_{H_n^0}^2,m_{\tilde t_i}^2)+\sum_{i,n=1}^{2}\lambda^2_{H_n^+\tilde t_L\tilde b_L}B_0(p^2,m_{H_n^+}^2,m_{\tilde b_L}^2)\ ,
\end{aligned}
\tag{C.3}
$$

$$
\begin{aligned}
16\pi^2\,\Pi_{\tilde t_R\tilde t_R}(p^2) &= \frac{8g_3^2}{3}\Big\{G(p^2,m_{\tilde g}^2,m_t^2)+s_t^2\Big[A_0(m_{\tilde t_1}^2)-(p^2+m_{\tilde t_1}^2)B_0(p^2,m_{\tilde t_1}^2,0)\Big]\\
&+ c_t^2\Big[A_0(m_{\tilde t_2}^2)-(p^2+m_{\tilde t_2}^2)B_0(p^2,m_{\tilde t_2}^2,0)\Big]\Big\}\\
&+ h_t^2\Big[c_t^2A_0(m_{\tilde t_1}^2)+s_t^2A_0(m_{\tilde t_2}^2)+A_0(m_{\tilde b_L}^2)\\
&+ \frac{1}{2}\sum_{n=1}^{4}D_nA_0(m_{H_n^0}^2)+\sum_{n=1}^{2}D_{n+2}A_0(m_{H_n^+}^2)+G(p^2,\mu^2,m_t^2)+G(p^2,\mu^2,m_b^2)\Big]\\
&+ \sum_{n=1}^{4}\sum_{i=1}^{2}\lambda^2_{H_n^0\tilde t_R\tilde t_i}B_0(p^2,m_{H_n^0}^2,m_{\tilde t_i}^2)+\sum_{i,n=1}^{2}\lambda^2_{H_n^+\tilde t_R\tilde b_L}B_0(p^2,m_{H_n^+}^2,m_{\tilde b_L}^2)\ , \qquad \text{(C.4)}
\end{aligned}
$$

$$
\begin{aligned}
16\pi^2\,\Pi_{\tilde t_L\tilde t_R}(p^2) &= \frac{4g_3^2}{3}\Big[-2(p^2+m_{\tilde t_1}^2)B_0(p^2,m_{\tilde t_1}^2,0)+2(p^2+m_{\tilde t_2}^2)B_0(p^2,m_{\tilde t_2}^2,0)\\
&+ 4m_{\tilde g}m_tB_0(p^2,m_{\tilde g}^2,m_t^2)\Big]+\frac{3}{2}h_t^2s_{2t}\Big[A_0(m_{\tilde t_1}^2)-A_0(m_{\tilde t_2}^2)\Big]\\
&+ \sum_{n=1}^{4}\sum_{i=1}^{2}\lambda_{H_n^0\tilde t_L\tilde t_i}\lambda_{H_n^0\tilde t_R\tilde t_i}B_0(p^2,m_{H_n^0}^2,m_{\tilde t_i}^2)\\
&+ \sum_{i,n=1}^{2}\lambda_{H_n^+\tilde t_L\tilde b_L}\lambda_{H_n^+\tilde t_R\tilde b_L}B_0(p^2,m_{H_n^+}^2,m_{\tilde b_L}^2)\ , \qquad \text{(C.5)}
\end{aligned}
$$

where $\lambda_{H^0\tilde t_L\tilde t_1} = c_t\lambda_{H^0\tilde t_1\tilde t_1} - s_t\lambda_{H^0\tilde t_2\tilde t_1}$, $\lambda_{H^0\tilde t_R\tilde t_1} = s_t\lambda_{H^0\tilde t_1\tilde t_1} + c_t\lambda_{H^0\tilde t_2\tilde t_1}$, *etc.*. The symbols D_n are defined after (B.7).

From (C.3-C.5) we derive relations between running and on-shell top-squark masses and mixing parameters using the following one-loop relationships (for $c_t^2 = s_t^2 = 1/2$):

$$
\begin{aligned}
M_{\tilde t_1}^2 &= M_Q^2+m_t^2+m_tX_t-\frac{1}{2}\mathrm{Re}\left[\Pi_{\tilde t_L\tilde t_L}(M_{\tilde t_1}^2)+\Pi_{\tilde t_R\tilde t_R}(M_{\tilde t_1}^2)\right]-\mathrm{Re}\ \Pi_{\tilde t_L\tilde t_R}(M_{\tilde t_1}^2)\ ,\\
M_{\tilde t_2}^2 &= M_Q^2+m_t^2-m_tX_t-\frac{1}{2}\mathrm{Re}\left[\Pi_{\tilde t_L\tilde t_L}(M_{\tilde t_2}^2)+\Pi_{\tilde t_R\tilde t_R}(M_{\tilde t_2}^2)\right]+\mathrm{Re}\ \Pi_{\tilde t_L\tilde t_R}(M_{\tilde t_2}^2)\ , \qquad \text{(C.6)}
\end{aligned}
$$

we obtain (assuming again a common heavy SUSY scale M_S and leaving free the μ-parameter):

$$
\begin{aligned}
m_{\tilde t}^2(Q) &= M_{\tilde t}^2\Big\{1-\frac{g_3^2}{3\pi^2}\left(2-\ln\frac{M_S^2}{Q^2}\right)+\frac{3h_t^2}{32\pi^2}\Big[(\hat X_t^2s_\beta^2+\hat Y_t^2c_\beta^2)\left(2-\ln\frac{M_S^2}{Q^2}\right)\\
&+ c_\beta^2\left(1-\frac{\pi}{\sqrt3}\hat Y_t^2-\ln\frac{M_S^2}{Q^2}\right)\\
&+ \hat\mu^4\ln\hat\mu^2+(1-\hat\mu^2)\left(3-2\ln\frac{M_S^2}{Q^2}\right)-(1-\hat\mu^2)^2\ln(1-\hat\mu^2)\Big]\Big\}\ , \qquad \text{(C.7)}\\
m_tX_t(Q) &= M_tX_t^{\mathrm{OS}}+\frac{g_3^2}{12\pi^2}m_tM_S\Big[4(2-\ln\frac{M_S^2}{Q^2})+2\hat X_t\ln\frac{M_S^2}{Q^2}\Big]\\
&+ \frac{3h_t^2}{16\pi^2}m_t\Big\{(X_ts_\beta^2+Y_tc_\beta^2)\left(2-\ln\frac{M_S^2}{Q^2}\right)-\frac{\pi}{\sqrt3}Y_tc_\beta^2+X_t\left(1-\frac{3}{2}\ln\frac{M_S^2}{Q^2}\right)\\
&- \frac{1}{2}\Big[1-\hat\mu^2+\hat\mu^4\ln\hat\mu^2+(1-\hat\mu^4)\ln(1-\hat\mu^2)\Big]X_t\Big\}\ , \qquad \text{(C.8)}
\end{aligned}
$$

where we have used (A.7), (A.9) and the definition $\hat{Y}_t \equiv (A_t - \mu\tan\beta)/M_S$.
–W boson:

$$16\pi^2\ \Pi^T_{WW}(p^2) = 3g^2\Big\{2B_{22}(p^2,m_t^2,m_b^2)+\frac{1}{2}G(p^2,m_t^2,m_b^2)-2c_t^2\Big[B_{22}(p^2,m^2_{\tilde{t}_1},m^2_{\tilde{b}_L})-\frac{1}{4}A_0(m^2_{\tilde{t}_1})\Big]$$
$$- 2s_t^2\Big[B_{22}(p^2,m^2_{\tilde{t}_2},m^2_{\tilde{b}_L})-\frac{1}{4}A_0(m^2_{\tilde{t}_2})\Big]+\frac{1}{2}A_0(m^2_{\tilde{b}_L})\Big\}\ . \tag{C.9}$$

This gives (under the assumption of the simplified SUSY spectrum of Sec. 2, described already for previous self-energies)

$$v^2(Q)=\frac{4}{g^2}[M_W^2+\mathrm{Re}\ \Pi^T_{WW}(M_W^2)]=\frac{4M_W^2}{g^2}\left[1-\frac{h_t^2 s_\beta^2}{32\pi^2}\left(-6\ln\frac{m_t^2}{Q^2}+3+\hat{X}_t^2\right)\right]\ , \tag{C.10}$$

where we have neglected the external momentum in (C.9) and used (A.3-A.6).
–Higgs boson: We need only the difference

$$16\pi^2\left[\Pi_{hh}(m^2_{h^0})-\Pi_{hh}(0)\right] = 3h_t^2 m^2_{h^0} s^2_\beta\left[B_0(0,m_t^2,m_t^2)-4m_t^2\ \frac{d}{dp^2}B_0(p^2,m_t^2,m_t^2)\Big|_{p^2=0}\right]$$
$$+\ 3m^2_{h^0}\sum_{i,j}\lambda^2_{h^0\tilde{t}_i\tilde{t}_j}\ \frac{d}{dp^2}B_0(p^2,m^2_{\tilde{t}_i},m^2_{\tilde{t}_j})\Big|_{p^2=0}\ , \tag{C.11}$$

where $\lambda_{h\tilde{t}_i\tilde{t}_j}$ are defined in (B.6). Using (A.6) and (A.7) we get (19).

Appendix D: MSSM effective potential to the two-loop order

In this Appendix we present the MSSM effective potential for the (real) neutral components of the Higgs fields up to the two-loop level in the leading approximation (which neglects all dimensionless couplings except h_t and g_3). We first write the potential as

$$V(h_1,h_2) = V_{\mathrm{vac}}+V_0(h_1,h_2)+V_1(h_1,h_2)+V_2(h_1,h_2)\ , \tag{D.1}$$

where V_{vac} is a field-independent vacuum energy term[¶]. The tree-level potential V_0 is

$$V_0(h_1,h_2) = \frac{1}{2}(m^2_{H_1}+\mu^2)h_1^2+\frac{1}{2}(m^2_{H_2}+\mu^2)h_2^2+B_\mu h_1h_2\ , \tag{D.2}$$

which simply follows from substituting Eq. (B.2) into the MSSM Higgs sector scalar potential (B.1).

[¶]This term is a function of the soft-breaking parameters; it is needed for the invariance of the potential under a RG transformation.

The one-loop potential is well known and the $\mathcal{O}(\alpha_s\alpha_t)$ part of the two-loop potential was computed in [6]; we list them here for completeness and for future reference. The complete one-loop potential in Laudau gauge is[‖]

$$\begin{aligned}16\pi^2\ V_1(h_1,h_2) \ &= \ \sum_f N_c^f\Big[\sum_{i=1,2} H(m_{\tilde{f}_i}^2) - 2H(m_f^2)\Big] + 3H(m_W^2) + \frac{3}{2}H(m_Z^2) \\ &+ \ \frac{1}{2}\sum_{n=1}^{4} H(m_{H_n^0}^2) + \sum_{n=1}^{2} H(m_{H_n^+}^2) - 2\sum_{i=1}^{2} H(m_{\tilde{\chi}_i^+}^2) - \sum_{i=1}^{4} H(m_{\tilde{\chi}_i^0}^2)\ , \qquad \text{(D.3)}\end{aligned}$$

where f sums over all the (s)quarks and (s)leptons, N_c^f is the color factor, 3 for (s)quarks and 1 for (s)leptons. Following the leading approximation, we keep only the numerically important parts, *i.e.*, those from top (s)quarks. In Eq. (D.3), $\tilde{\chi}_i^+(i = 1,2)$ and $\tilde{\chi}_i^0(i = 1,2,3,4)$ represent charginos and neutralinos, and the function H is

$$H(m^2) = \frac{m^4}{2}\left(\ln\frac{m^2}{Q^2} - \frac{3}{2}\right)\ . \qquad \text{(D.4)}$$

The QCD contribution to the two-loop effective potential in the MSSM is

$$\begin{aligned}(16\pi^2)^2\ V_{2s}(h_1,h_2) \ &= \ 8g_3^2\Big\{J(m_t^2,m_t^2) - 2m_t^2\ I(m_t^2,m_t^2,0) \\ &+\frac{1}{2}(c_t^4+s_t^4)\sum_{i=1}^{2} J(m_{\tilde{t}_i}^2,m_{\tilde{t}_i}^2) + 2s_t^2c_t^2 J(m_{\tilde{t}_1}^2,m_{\tilde{t}_2}^2) + \sum_{i=1}^{2} m_{\tilde{t}_i}^2 I(m_{\tilde{t}_i}^2,m_{\tilde{t}_i}^2,0) \\ &+\sum_{i=1}^{2} L(m_{\tilde{t}_i}^2,m_{\tilde{g}}^2,m_t^2) - 4m_{\tilde{g}}\ m_t\ s_t c_t\Big[I(m_{\tilde{t}_1}^2,m_{\tilde{g}}^2,m_t^2) - I(m_{\tilde{t}_2}^2,m_{\tilde{g}}^2,m_t^2)\Big]\Big\}\ , \qquad \text{(D.5)}\end{aligned}$$

where $\tilde{g}$ is the gluino, with tree-level mass given by the $SU(3)$ gaugino soft mass M_3. The two-loop scalar functions I, J and L in Eq. (D.5) are given in Appendix A, Eqs. (A.17), (A.16) and (A.20).[**]

The top Yukawa contribution to the two-loop potential is a new result of this paper. The relevant Feynman diagrams are shown in Fig. 8. To simplify the final result, we neglect left-right mixings in the bottom-squark sector and the gaugino-Higgsino mixings in the neutralino-chargino sector (under this assumption, the Higgsino masses are simply $|\mu|$); these simplifications are valid in the leading approximation. Using the Feynman rules given in Appendix B, we find (the last diagram of Fig. 8 is of order h_t^2 but does not contribute to m_{h^0})

$$(16\pi^2)^2\ V_{2t}(h_1,h_2) \ = \ 3h_t^2\Big\{\sum_{n=1}^{4}\frac{D_n}{2}\Big[L(m_{H_n^0}^2,m_t^2,m_t^2) \pm 2m_t^2 I(m_{H_n^0}^2,m_t^2,m_t^2) + \sum_{i=1}^{2} J(m_{\tilde{t}_i}^2,m_{H_n^0}^2)\Big]$$

[‖]We adopt the (modified) $\overline{\mathrm{DR}}$ -scheme of Ref. [22].

[**]The procedure we have followed of subtracting all possible one-loop subdivergences to define these functions is an alternative to the direct way used in Ref. [5]. The direct way requires the computation of some one-loop quantities to order $\mathcal{O}(\epsilon)$; perhaps we find the subtraction method simpler. We have explicitly checked that, in the particular limit studied in [5], we exactly reproduce their unexpanded mass formula, Eq. (11) of [5], which shows the equivalence of both methods.

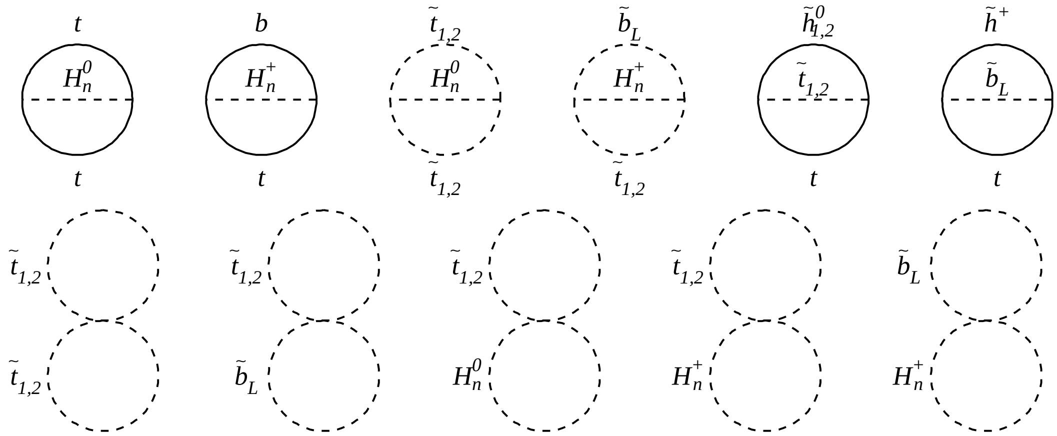

Figure 8: Feynman diagrams for the two-loop effective potential of order $\mathcal{O}(\alpha_t^2)$ in the MSSM. H_n^0 represent H^0, h^0, G^0 and A^0 for $n = 1, 2, 3, 4$. H_n^+ represent G^+, H^+ for $n = 1, 2$. The neutral and charged Higgsinos $\tilde{h}^0_{1,2}$ ($\equiv \tilde{\chi}^0_{3,4}$) and $\tilde{h}^+$ ($\equiv \tilde{\chi}^+_2$) have degenerate mass of $|\mu|$.

$$
\begin{aligned}
&+\sum_{n=1}^{2} D_{n+2}\Big[L(m^2_{H_n^+}, m_t^2, m_b^2) + s_t^2 J(m^2_{\tilde{t}_1}, m^2_{H_n^+}) + c_t^2 J(m^2_{\tilde{t}_2}, m^2_{H_n^+}) + J(m^2_{\tilde{b}_L}, m^2_{H_n^+})\Big] \\
&+s_t^2 J(m^2_{\tilde{t}_1}, m^2_{\tilde{b}_L}) + c_t^2 J(m^2_{\tilde{t}_2}, m^2_{\tilde{b}_L}) + s_{2t}^2 \sum_{i=1}^{2} J(m^2_{\tilde{t}_i}, m^2_{\tilde{t}_i}) + c_{4t} J(m^2_{\tilde{t}_1}, m^2_{\tilde{t}_2}) \\
&+\sum_{i=1}^{2} L(m^2_{\tilde{t}_i}, \mu^2, m_t^2) + L(m^2_{\tilde{b}_L}, \mu^2, m_t^2) + s_t^2 L(m^2_{\tilde{t}_1}, \mu^2, m_b^2) + c_t^2 L(m^2_{\tilde{t}_2}, \mu^2, m_b^2)\Big\} \\
&-\frac{3}{2}\sum_{i,j=1}^{2}\sum_{n=1}^{4} \lambda^2_{H_n^0 \tilde{t}_i \tilde{t}_j} I(m^2_{H_n^0}, m^2_{\tilde{t}_i}, m^2_{\tilde{t}_j}) - 3\sum_{i,j=1}^{2}\sum_{n=1}^{2} \lambda^2_{H_n^+ \tilde{t}_i \tilde{b}_L} I(m^2_{H_n^+}, m^2_{\tilde{t}_i}, m^2_{\tilde{b}_L}) \ , \qquad \text{(D.6)}
\end{aligned}
$$

where in the first line of Eq. (D.6), positive and negative signs apply to $\mathcal{CP}$-even (H^0, h^0) and odd (A^0, G^0) Higgs/Goldstone bosons respectively. The Higgs/Goldstone-squark couplings are defined in Eq. (B.6) while the D_n symbols are defined after Eq. (B.7).

Two tests can be applied to check the correctness of the effective potential $V(h_1, h_2)$. First, the potential should vanish in the supersymmetric limit (*i.e.*, when all soft-breaking parameters are taken to be zero), and second, the potential $V(h_1, h_2)$ should be invariant under changes of the renormalization scale, up to the order of our perturbative calculation. The vanishing of the potential in the supersymmetric limit is proved by simple algebra. In the following we show the invariance of the two-loop potential under a RG transformation.

Using the derivatives of I, J and L functions with respect to the renormalization scale Q

$$
\frac{\partial I(m_1^2, m_2^2, m_3^2)}{\partial \ln Q^2} = -\sum_{i=1}^{3}\Big[A_0(m_i^2) + m_i^2\Big] \ , \qquad \text{(D.7)}
$$

$$
\frac{\partial J(m_1^2, m_2^2)}{\partial \ln Q^2} = m_1^2 A_0(m_2^2) + m_2^2 A_0(m_1^2) \ , \qquad \text{(D.8)}
$$

$$
\frac{\partial L(m_1^2, m_2^2, m_3^2)}{\partial \ln Q^2} = (m_1^2 - 2m_2^2 - 2m_3^2) A_0(m_1^2) - m_2^2 A_0(m_2^2) - m_3^2 A_0(m_3^2)
$$

$$+ m_1^4 - (m_2^2 + m_3^2)^2 \ , \tag{D.9}$$

and the one-loop MSSM RGEs for top-(s)quark and Higgs boson masses, Eqs. (B.12-B.16), we find that the RG variation

$$\begin{aligned} -\frac{\partial V_2}{\partial \ln Q^2} - \mathcal{D}^{(1)} V_1 &= \frac{8 g_3^2 h_t^2 h_2^2}{(16\pi^2)^2} \Big(M_{\widetilde{Q}}^2 + M_{\widetilde{U}}^2 + 2 M_3^2 + X_t^2 - 2 M_3 X_t \Big) \\ &- \frac{9 h_t^4 h_2^2}{(16\pi^2)^2} \Big\{ M_{\widetilde{Q}}^2 + M_{\widetilde{U}}^2 + \frac{1}{2} \Big[m_{H_2}^2 + (A_t + X_t)^2 \Big] \Big\} \end{aligned} \tag{D.10}$$

modulo terms independent of the Higgs field h_2. Here $\mathcal{D}^{(1)} V_1$ represents the one-loop RG variation of the one-loop potential Eq. (D.3). This result agrees exactly with the two-loop RG variation of the tree-level potential $\mathcal{D}^{(2)} V_0$ [*cf.* Eqs. (D.2) and (B.9-B.11)], so that

$$\frac{d}{d \ln Q^2} (V_0 + V_1 + V_2) \equiv \mathcal{D}^{(2)} V_0 + \mathcal{D}^{(1)} V_1 + \frac{\partial V_2}{\partial \ln Q^2} = 0 \ . \tag{D.11}$$

Note that this is a nontrivial check that all $\ln Q^2$ terms cancel with each other between Eq. (D.10) and $\mathcal{D}^{(2)} V_0$; this cancellation guarantees the correct leading and next-to-leading order logarithmic behavior of the effective potential.

To derive the analytical expression of $\Delta m_{h^0}^2$ in Sec. 2, we need to expand the two-loop potential V_2 in powers of m_t/M_S and $m_t X_t/M_S^2$; besides many straightforward expansions, we have used (A.25)-(A.28) for the $t - \tilde{q} - \tilde{h}$ and $\tilde{t} - \tilde{q} - h$ diagrams of (D.6), with $\tilde{q} = \tilde{t}$ or $\tilde{b}$.

References

[1] For reviews, see *e.g.*
H. P. Nilles, *Phys. Rep.* **110** (1984) 1;
H. E. Haber and G. L. Kane, *Phys. Rep.* **117** (1985) 75.

[2] LEP Experiments Committee Meeting, March 7th, 2000,
`http://alephwww.cern.ch/ALPUB/seminar/lepc_mar2000/LEPC2000_files/v3_document.htm`;
`http://delphiwww.cern.ch/~offline/physics_links/lepc.html`;
`http://l3www.cern.ch/analysis/latestresults.html`;
`http://www.cern.ch/Opal/PPwelcome.html`.

[3] S. P. Li and M. Sher, *Phys. Lett.* **B140** (1984) 339;
J. Ellis, G. Ridolfi and F. Zwirner, *Phys. Lett.* **B257** (1991) 83; *ibid.* **262** (1991) 477;
Y. Okada, M. Yamaguchi, and T. Yanagida, *Prog. Theor. Phys.* **85** (1991) 1;
D. M. Pierce, A. Papadopoulos and S. B. Johnson, *Phys. Rev. Lett.* **68** (1992) 3678;
M. Drees and M. M. Nojiri, *Phys. Rev.* **D45** (1992) 2482;
A. V. Gladyshev, D. I. Kazakov, W. de Boer, G. Burkart and R. Ehret, *Nucl. Phys.* **B498** (1997) 3.

[4] J. A. Casas, J. R. Espinosa, M. Quirós and A. Riotto, *Nucl. Phys.* **B436** (1995) 3.

[5] R. Hempfling and A. H. Hoang, *Phys. Lett.* **B331** (1994) 99.

[6] R.-J. Zhang, *Phys. Lett.* **B447** (1999) 89.

[7] J. R. Espinosa and R.-J. Zhang, `hep-ph/9912236`.

[8] M. S. Berger, *Phys. Rev.* **D41** (1990) 225;
H. E. Haber and R. Hempfling, *Phys. Rev. Lett.* **66** (1991) 1815;
M. A. Díaz and H. E. Haber, *Phys. Rev.* **D46** (1992) 3086;
P. H. Chankowski, S. Pokorski and J. Rosiek, *Phys. Lett.* **B274** (1992) 191; *Nucl. Phys.* **B423** (1994) 437;
A. Yamada, *Phys. Lett.* **B263** (1991) 233; *Z. Phys.* **C61** (1994) 247;
A. Brignole, *Phys. Lett.* **B281** (1992) 284;
A. Dabelstein, *Z. Phys.* **C67** (1995) 495.

[9] S. Heinemeyer, W. Hollik and G. Weiglein, *Phys. Rev.* **D58** (1998) 091701; *Phys. Lett.* **B440** (1998) 296; *Eur. Phys. J.* **C9** (1999) 343.

[10] D. M. Pierce, J. A. Bagger, K. T. Matchev and R.-J. Zhang, *Nucl. Phys.* **B491** (1997) 3.

[11] R. Barbieri, M. Frigeni and M. Caravaglios, *Phys. Lett.* **B258** (1991) 167;
Y. Okada, M. Yamaguchi, and T. Yanagida, *Phys. Lett.* **B262** (1991) 54;
J. R. Espinosa and M. Quirós, *Phys. Lett.* **B266** (1991) 389;
K. Sasaki, M. Carena and C. E. M. Wagner, *Nucl. Phys.* **B381** (1992) 66;
H. E. Haber and R. Hempfling, *Phys. Rev.* **D48** (1993) 4280.

[12] M. Carena, J. R. Espinosa, M. Quirós and C. E. M. Wagner, *Phys. Lett.* **B355** (1995) 209;
M. Carena, M. Quirós and C. E. M. Wagner, *Nucl. Phys.* **B461** (1996) 407.

[13] H. E. Haber, R. Hempfling and A. H. Hoang, *Z. Phys.* **C75** (1997) 539.

[14] M. Carena, H. E. Haber, S. Heinemeyer, W. Hollik, C. E. M. Wagner and G. Weiglein, `hep-ph/0001002`.

[15] D. Comelli and J. R. Espinosa, *Phys. Lett.* **B388** (1996) 793.

[16] A. Sirlin and R. Zucchini, *Nucl. Phys.* **B266** (1986) 389.

[17] S. Heinemeyer, W. Hollik and G. Weiglein, *Comp. Phys. Commun.* **124** (2000) 76.

[18] S. Coleman and E. Weinberg, *Phys. Rev.* **D7** (1973) 1888;
R. Jackiw, *Phys. Rev.* **D9** (1974) 1686.

[19] C. Ford, and D. R. T. Jones, *Phys. Lett.* **B274** (1992) 409, Erratum-*ibid.* **B285** (1992) 399;
C. Ford, I. Jack and D. R. T. Jones, *Nucl. Phys.* **B387** (1992) 373, Erratum-*ibid.* **B504** (1997) 551.

[20] M. Caffo, H. Czyż, S. Laporta and E. Remiddi, *Nuovo Cim.* **111A** (1998) 365.

[21] A. I. Davydychev and J. B. Tausk, *Nucl. Phys.* **B397** (1993) 123;
A. I. Davydychev, V. A. Smirnov and J. B. Tausk, *Nucl. Phys.* **B410** (1993) 325;
F. A. Berends and J. B. Tausk, *Nucl. Phys.* **B421** (1994) 456.

[22] W. Siegel, *Phys. Lett.* **B84** (1979) 19;
D. M. Capper, D. R. T. Jones and P. van Nieuwenhuizen, *Nucl. Phys.* **B167** (1980) 479;
I. Jack, D. R. T. Jones, S. P. Martin, M. T. Vaughn and Y. Yamada, *Phys. Rev.* **D50** (1994) 5481.

[23] K. Inoue, A. Kakuto, H. Komatsu and S. Takeshita, *Prog. Theor. Phys.* **68** (1982) 927; *ibid.* **71** (1984) 413;
S. P. Martin and M. T. Vaughn, *Phys. Rev.* **D50** (1994) 2282;
Y. Yamada, *Phys. Rev.* **D50** (1994) 3537;
I. Jack and D. R. T. Jones, *Phys. Lett.* **B333** (1994) 372.

[24] A. Donini, *Nucl. Phys.* **B467** (1996) 3.